TECHNICAL REPORT BRL-TR-3102

BRL

NEW DIRECTIONS IN MULTIPHASE FLOW INTERIOR BALLISTIC MODELING

ALBERT W. HORST
GEORGE E. KELLER
PAUL S. GOUGH

MAY 1990

U.S. ARMY LABORATORY COMMAND

BALLISTIC RESEARCH LABORATORY
ABERDEEN PROVING GROUND, MARYLAND

NOTICES

Destroy this report when it is no longer needed. DO NOT return it to the originator.

Additional copies of this report may be obtained from the National Technical Information Service, U.S. Department of Commerce, 5285 Port Royal Road, Springfield, VA 22161.

The findings of this report are not to be construed as an official Department of the Army position, unless so designated by other authorized documents.

The use of trade names or manufacturers' names in this report does not constitute indorsement of any commercial product.

UNCLASSIFIED

REPORT DOCUMENTATION PAGE

Form Approved
OMB No. 0704-0188

1. AGENCY USE ONLY (Leave blank)	2. REPORT DATE	3. REPORT TYPE AND DATES COVERED
	MAY 90	TR Oct 86 - Sep 89

4. TITLE AND SUBTITLE
New Directions in Multiphase Flow Interior Ballistic Modeling

5. FUNDING NUMBERS
1L161102AH43

6. AUTHOR(S)
Albert W. Horst, George E. Keller and Paul S. Gough

7. PERFORMING ORGANIZATION NAME(S) AND ADDRESS(ES)

8. PERFORMING ORGANIZATION REPORT NUMBER

9. SPONSORING / MONITORING AGENCY NAME(S) AND ADDRESS(ES)
USA Ballistic Research Laboratory
ATTN: SLCBR-DD-T
Aberdeen Proving Ground, MD 21005-5066

10. SPONSORING / MONITORING AGENCY REPORT NUMBER
BRL-TR-3102

11. SUPPLEMENTARY NOTES

12a. DISTRIBUTION / AVAILABILITY STATEMENT
Approved for public release; distribution is unlimited.

superscript n

12b. DISTRIBUTION CODE

13. ABSTRACT (Maximum 200 words)

Over the past two decades, several two-phase-flow interior ballistic codes have been developed. Generally, they have treated ignition-induced pressure waves as a hydrodynamic problem which arises from the ignition stimulus, the propellant geometry, the path of flamespreading in the propellant bed, and the interaction of charge and chamber. Ignition and combustion have been treated as a simple process, with convectively-driven inert heating of the propellant until a surface-temperature criterion is reached, at which time an aP^n burning law describes the propellant surface regression, and all of the energy contained in the burned propellant is released immediately. The effects of propellant grain fracture, caused either by grain stress due to propellant bed compaction or by impact with fixed boundaries, has been outside the scope of the several codes. While the codes have incorporated interphase heat transfer and drag, they have been called "inviscid", as the conservation laws are formulated to neglect the efforts of viscosity and heat conduction in the gas phase.

This report describes, for the NOVA family of codes, a) the recent inclusion of finite-rate chemistry and grain fracture, b) planned efforts to improve the propellant near-field combustion model further, and c) ongoing efforts to formulate a viscid/inviscid model to permit a linkage of effects with widely differing scales of heterogeneity. Keywords

14. SUBJECT TERMS
Interior Ballistics, Modeling, Kinetics, Viscosity

15. NUMBER OF PAGES
54

16. PRICE CODE

17. SECURITY CLASSIFICATION OF REPORT	18. SECURITY CLASSIFICATION OF THIS PAGE	19. SECURITY CLASSIFICATION OF ABSTRACT	20. LIMITATION OF ABSTRACT
UNCLASSIFIED	UNCLASSIFIED	UNCLASSIFIED	SAR

INTENTIONALLY LEFT BLANK.

TABLE OF CONTENTS

INTENTIONALLY LEFT BLANK.

LIST OF FIGURES

INTENTIONALLY LEFT BLANK.

I. HISTORICAL PERSPECTIVE

Over the past two decades, the field of interior ballistic modeling has undergone a number of major advances. Early lumped-parameter models, which appeared in abundance as computer codes[1] in the mid-1960's, provide the charge designer with powerful tools to perform large, parametric interior ballistic studies rapidly and efficiently. These codes embody such assumptions as uniform and instantaneous ignition of the entire propellant charge, with combustion taking place in a smoothly varying, well-stirred mixture, the burning rate being determined by the instantaneous, "space-mean" gas pressure. A pressure gradient within the gun tube is typically superimposed on this solution to provide an appropriately reduced projectile base pressure, but these codes cannot address the physical hydrodynamics of the problem as manifested in ignition-induced pressure waves. Nonetheless, lumped-parameter codes have been and are still used throughout the world for most basic interior ballistic systems and charge design studies. For example, propellant thermochemical codes have been used in conjunction with lumped-parameter interior ballistic codes in expert systems for solution of the overall propellant formulation/charge design optimization problem.[2] However, the prevalence of gun malfunctions, the origins of which were ultimately traced to ignition-related pressure waves,[3,4] motivated serious development of multiphase flow interior ballistic models beginning in the early 1970's.

First on the scene were one-dimensional, two-phase flow models,[5-7] the primary purpose of which was to assess the influence of the ignition stimulus on flamespreading and the formation of pressure waves. At least in the US, probably the most successful and certainly the most used of such models has been the NOVA code,[8] developed and advanced by Paul Gough Associates in conjunction with the US Naval Ordnance Station, Indian Head, Maryland and the US Army Ballistic Research Laboratory, Aberdeen Proving Ground, Maryland, initially in response to pressure-wave problems experienced in Navy 5-inch guns and Army 155-mm howitzers. NOVA provides a macroscopic, two-phase flow treatment of the gun interior ballistic cycle, formulated under the assumption of quasi-one-dimensional flow. It is commonly called an "inviscid" model, as the conservation laws are formulated to neglect the effects of viscosity and heat conduction in the gas phase. Essential to the model, however, is the coupling of the gas and solid phases through heat transfer, combustion, and interphase drag; these exchange processes are modeled via empirical correlations relating complex microphenomena to the average flow properties described in the governing equations. Functioning of the igniter is included by specifying a predetermined mass injection rate as a function of position and time, along with appropriate thermochemical information for conversion of the mass into hot gas and/or hot, condensed phase material. Flamespreading is driven by axial convection, the propellant responding as an inert substance until a predetermined surface temperature is reached. Propellant combustion then follows the same pressure-dependent description typically used in lumped-parameter codes - this time, however, with a locally prescribed rate dependent on the local instantaneous pressure. (Several other ignition and combustion options are available in some versions of the code to account for transient and erosive contributions but remain largely untested.) In addition, internal boundaries defined by discontinuities in porosity are treated explicitly, and a lumped-parameter treatment is included to reflect the inertial and compactibility characteristics of any inert packaging elements (e.g., case closure plugs) present between the propellant bed and the base of

the projectile. Numerous successful applications of this code are described in the literature.[9,10]

Next in the progression of US modeling efforts were several quasi-two-dimensional treatments,[11,12] in which coaxial regions of propellant and circumferential ullage are treated as coupled regions of one-dimensional flow. Thus, the influence of ullage external to a bagged artillery charge on the path of flamespreading and the equilibration of pressure gradients can be estimated. Other aspects of the modeling are, however, in basic agreement with that of NOVA, including the simple surface temperature ignition criterion and the global, pressure-dependent combustion process assumed to occur at the propellant surface.

More recently, emphasis has been placed on fully two-dimensional interior ballistic models. TDNOVA[13-16] provides an axisymmetric description of macroscopic flow and includes many special features to model the fluid dynamics particular to stick propellants and rigidized combustible cases. A great deal of success modeling both granular and stick propellant artillery charges has been achieved with this code.[16-18] However, the emphasis of such efforts was on increasing the fidelity of the treatment of the configural complexities of the propelling charge and gun chamber within the limitations of an "inviscid" representation.

Concurrent with these efforts to develop and apply multidimensional codes, a considerable effort was also expended to increase the utility of existing one-dimensional formulations. Extensions to NOVA included a) a dual-voidage treatment of stick propellant, b) independently treating gas-phase variables in the perforations and in the interstices between sticks, as well as c) heat transfer to, ignition, and surface regression for interior and exterior surfaces of the sticks.[19] Other problems addressed include traveling charges, control tube primers, and various, complicated loading arrangements of multiple propellant charges.[20]

The authors would be remiss in closing this brief review if mention were not made of the considerable body of work that has been performed by investigators, largely outside the propelling charge design community, who have focused on providing a full Navier-Stokes description of flow in a gun tube, with particular attention on the development of the unsteady boundary layer and heat transfer to the tube. The DELTA code in the US[21], the EMI code in Germany,[22] as well as many other models,[23-26] appear in the literature throughout the free world. To date, however, such efforts almost universally address the single-phase problem (the all-burnt "Lagrange problem") or a two-phase problem in which the solid phase is a finely dispersed particulate, thereby avoiding the problem of conflict in scales that would result from the simultaneous treatment recognizing propellant grains whose critical dimensions are of the same scale or even larger than those of the boundary layer. Substantial progress beyond this point awaits the availability of computers large and fast enough to solve the detailed flow problem around and among the thousands of propellant grains present in a typical granular charge, or perhaps a more innovative approach.

Throughout the course of the efforts outlined above, areas of investigation and code improvements were pursued in response to two stimuli. The first was the existence of particular, exigent needs of the charge design community, such as specific new performance requirements or the occurrence of ammunition malfunctions. Such motivators occur irregularly, but with priority and usually funding as well! The second is the more academically pleasing search for a more phenomenologically complete interior ballistic model, embodying everything we know about all aspects of the interior ballistic cycle and consistent with current computational capabilities.

The paramount responsibility of the interior ballistic modeler, however, is to combine appropriately detailed submodels (e.g., ignition, combustion, mechanical properties, fluid dynamics) so that their interactions within the overall interior ballistic model provide an increased predictive or diagnostic capability. It is in the spirit of a positive response to both the problems facing the charge design community and the responsibility of the interior ballistic modeler that we have focused our attentions on the new modeling thrusts described in this report.

II. SUMMARY OF NEW AREAS OF EMPHASIS

A. Improved Kinetics for Two-Phase Flow Models

1. Background. An emphasis on hydrodynamics until recently has resulted not from a lack of interest in the ignition and combustion processes themselves but rather from a belief that no real progress could be made in modeling flamespreading and pressure-wave phenomena in real-world charges until an overall modeling framework was established which recognized the associated configural complexities of the problem. With rugged versions of NOVA and TDNOVA representing a major step toward providing this capability, we turned to the next level of deficiencies appearing to impede serious progress - the vastly simplified picture of propellant ignition and combustion employed by most such codes.

Ample evidence, in the form of long ignition delays (tens to hundreds of milliseconds for the low-pressure artillery ignition event), first luminosity and apparent gas-phase reactivity in regions of ullage downstream from the propellant bed, and unexpected vigorous combustion events often occurring after long ignition delays, suggests the presence of finite-rate kinetics outside the scope of most interior ballistic models.[27,28] The concern over finite-rate kinetics has been heigntened by the advent of LOVA (low-vulnerability) gun propellants, which often reveal disparities, sometimes large, between calculated and experimental performance. The very nature of low-vulnerability propellants makes them more difficult to ignite, a feature that can influence the rate of flamespreading and overall performance as well.[29]

The combustion mechanism for LOVA propellants, particularly at low pressures, may in no way resemble a simple, global reaction at the propellant surface. Early binder decomposition yielding fuel-rich products may yield likely candidates for subsequent gas-phase reactions, which themselves can have significant impact on both flamespreading and ensuing ballistic processes. To investigate a broad range of such interactions, a rugged and computationally efficient version of the NOVA code was modified to include a number of revisions to the ignition and combustion submodels.[20]

2. The XNQVAKTC Representation. The ignition model was extended to treat igniters whose products of combustion constitute a multiphase, reacting, homogeneous mixture of an arbitrary number of chemical species, with a similarly arbitrary number of chemical reactions admitted among them. Igniter output is still modeled as a mass flux, but condensed phases may be deposited directly on the propellant surface, significantly enhancing heat transfer, while altering the mixture of igniter products remaining in the flow. In the code, the rate of deposition of condensed igniter products onto the surface of the solid propellant is proportional to the concentration of the solid propellant and the relative momentum flux of the mixture of combustion products.

Upon "ignition" of the main propellant charge, the mass generated as a result of local decomposition is not assumed to consist of final products of combustion. Rather, an arbitrary number of intermediate products are assumed, and release of full energy of combustion occurs only after further chemical reaction in the mixture, a process that may include chemical interaction with the igniter products as well (see Figure 1).

All reactions are assumed to have rates governed by a general Arrhenius law. Each reaction is assumed to proceed in the forward direction only:

$$\sum_{i=o}^{n} \nu_{ik}' \, S_i \rightarrow \sum_{i=o}^{n} \nu_{ik}'' \, S_i \quad ,$$

where S_i represents species i, and ν_{ik}', and ν_{ik}'' are the stoichiometric coefficients for reactants and products respectively. (The summation is extended to include $i=o$ to incorporate formally a reaction with a spectator molecule.) The rate of reaction k is r_k, where

$$r_k = B_k \, T^{\beta_k} \exp\left[-\frac{E_k}{R_u \, T}\right] \prod_{i=o}^{N} (Y_i \rho)^{\nu_{ik}'''} \quad .$$

We note that the reactions order of ν_{ik}''' may differ from that of ν_{ik}', since for many applications of interest, reaction k will be a global rather than an elemental reaction. The rate of production of species i by reaction k is

$$r_{ik} = (\nu_{ik}'' - \nu_{ik}') r_k \quad ,$$

per unit volume of the mixture.

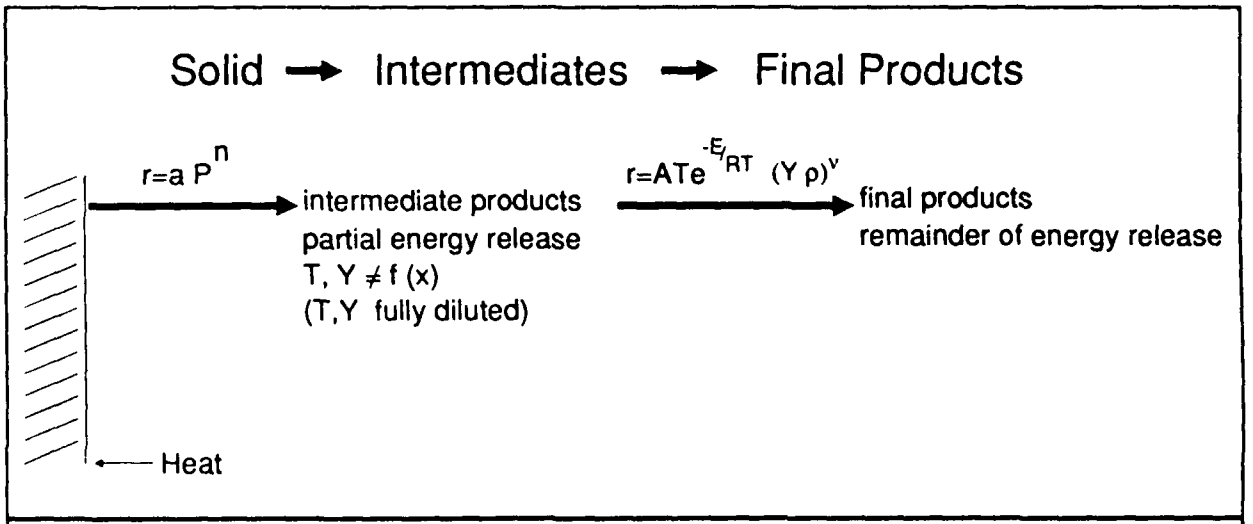

Figure 1. Schematic of Combustion Submodel in XNOVAKTC

3. Application. Initial application of this code has been made to the problem of a US 105-mm tank gun firing a candidate LOVA propellant.[30] Firing data had revealed significant differences in performance as a function of igniter alone, with increases in pressure and velocity of over 30% and 10% respectively when using igniters whose products of combustion were expected to be rich in available oxygen. Certainly one interpretation of these results is that the igniter products participated chemically in the combustion, as well as the ignition, of the main LOVA propellant charge.

In this study using XNOVAKTC, the modified version of the NOVA code, two different simple kinetic schemes were investigated. (A complete listing of input data is provided in Appendix A.) In both cases, convective ignition of the main charge was computed locally, with subsequent propellant regression defined by a simple aP^n burning rate law, with only half of the total chemical energy available from complete combustion being released at or near the surface; the balance of the energy was available for release later in flame zone or gas-phase reactions.

In the first scheme, regression produced a gaseous species which we called LOVA-I, an "intermediate state" associated with combustion of the particular propellant, which then further reacted upon collision with any gaseous species to form LOVA-F, the final gaseous state, and released the other half of its available energy.

The results summarized in Table 1 characterize the rate dependence of predicted ballistic results, for an activation energy and a range of pre-exponential factors based on the suggestions of Price[31] and based on work done at the Naval Weapons Center, China Lake, CA.[32-35] In this case, there were four gaseous species: air, igniter gas, LOVA-I, and LOVA-F; a collision with any one of them had the same potential for reaction. The table thus defines the range of pre-exponential factors necessary for transition from nearly no reaction to nearly complete reaction of intermediate to final combustion products, with substantial impact on predicted performance.

A second scheme investigated the effects of one additional reaction, one between the LOVA-I's and the igniter gases, allowing the chemical interaction of the igniter products with the main charge intermediate state, as postulated earlier in the possible explanation for the observed 105-mm firing data. Table 2 summarizes results for this two-reaction scheme for a situation in which the first reaction would have left about half of the LOVA-I intermediates unreacted, but the second reaction hastened the conversion and restored much of the full performance of the system.

The influence of these two schemes on the evolution of gaseous species is shown in Figures 2 and 3; a full discussion of the problem is provided in the reference.[30] For Figure 2, B = 5.25E5 cm^3/g-s. For Figure 3, B(2) = 5.25E7 cm^3/g-s.

Table 1. Performance Predictions Based on One Gas-Phase Reaction

LOVA-I + M -> LOVA-F + M

B = pre-exponential factor
E = activation energy = 7.5E4 Joules/mole

B (cm^3/g-s)	Peak Pressure (MPa)	Muzzle Velocity (m/s)	LOVA-F/LOVA-Total at Muzzle
1.05E5	123.6	653	0.003
5.25E5	154.9	801	0.504
1.05E6	337.9	1147	0.972
5.25E6	439.5	1229	0.997
5.25E7	446.1	1235	0.9997

Table 2. Performance Predictions Based on Two Gas-Phase Reactions

(1) LOVA-I + M -> LOVA-F + M

B(1) = 5.25E5 cm^3/g-s
E(1) = 7.5E4 Joules/mole

(2) LOVA-I + Igniter(G) -> LOVA-F + Air

E(2) = 7.5E4 Joules/mole

B (cm^3/g-s)	Peak Pressure (MPa)	Muzzle Velocity (m/s)	LOVA-F/LOVA-Total at Muzzle
5.25E5	160.8	824	0.567
5.25E6	235.8	999	0.825
5.25E7	362.8	1161	0.934
5.25E8	422.2	1218	0.980

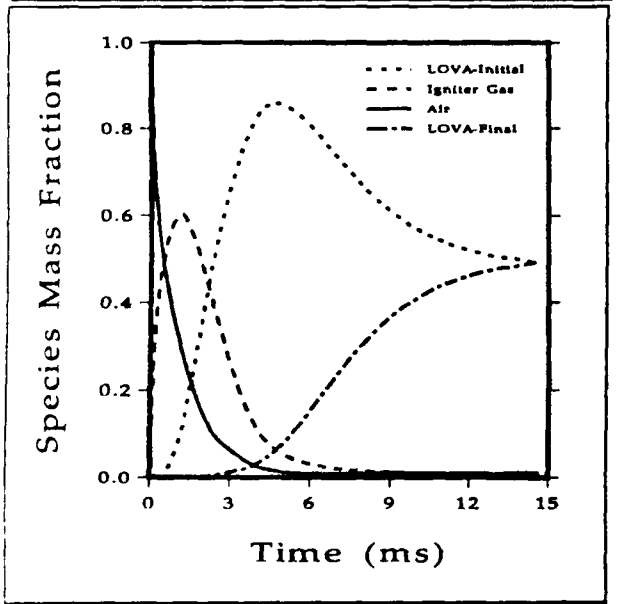

Figure 2. Evolution of Gaseous Species for One Gas-Phase Reaction

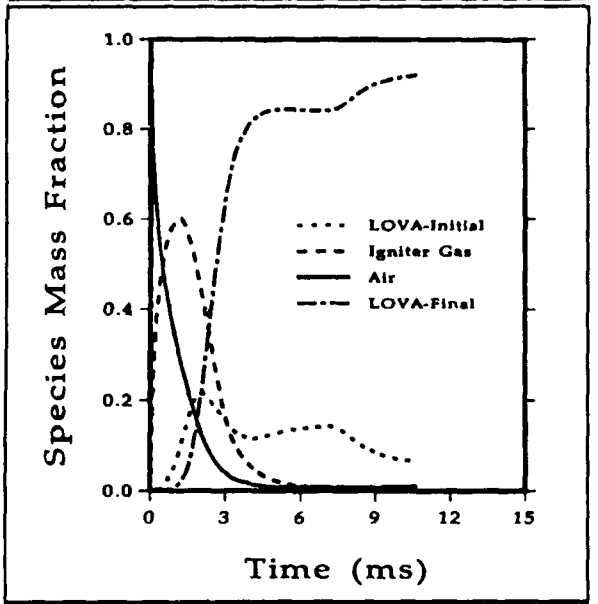

Figure 3. Evolution of Gaseous Species for Two Gas-Phase Reactions

4. Future Extensions. A serious limitation of the current approach finds its source in the macroscopic length scale, which divides the flow into two disjoint regions - the solid propellant and the products of combustion - and takes the contents of each of the regions to be locally homogeneous. Intermediate products of combustion are instantaneously mixed with the local ambient and are thermally equilibrated. The rate of reactions is therefore computed under conditions of possible dilution and incorrect temperature. Future representations must characterize all major reaction zones - subsurface, near-field, and far-field, requiring an extension to the analysis of a second length scale, namely the microscopic. Currently, the behavior of the gas-phase is driven by an empirical heat transfer correlation supplemented by the Zel'dovich formulation[36] of the heat feedback from the flame. No matter what happens beneath the surface and no matter what the ambient pressure and temperature, it is assumed that the local decomposition products remain the same and release the same fraction of the chemical energy of the propellant.

A near-field combustion model could be introduced into XNOVAKTC by providing an explicit representation of the microstructure within the gas phase adjacent to the surface of the solid propellant (see Figure 4). By explicitly modeling the temperature and species concentrations between the surface of the propellant and asymptotic boundaries whose

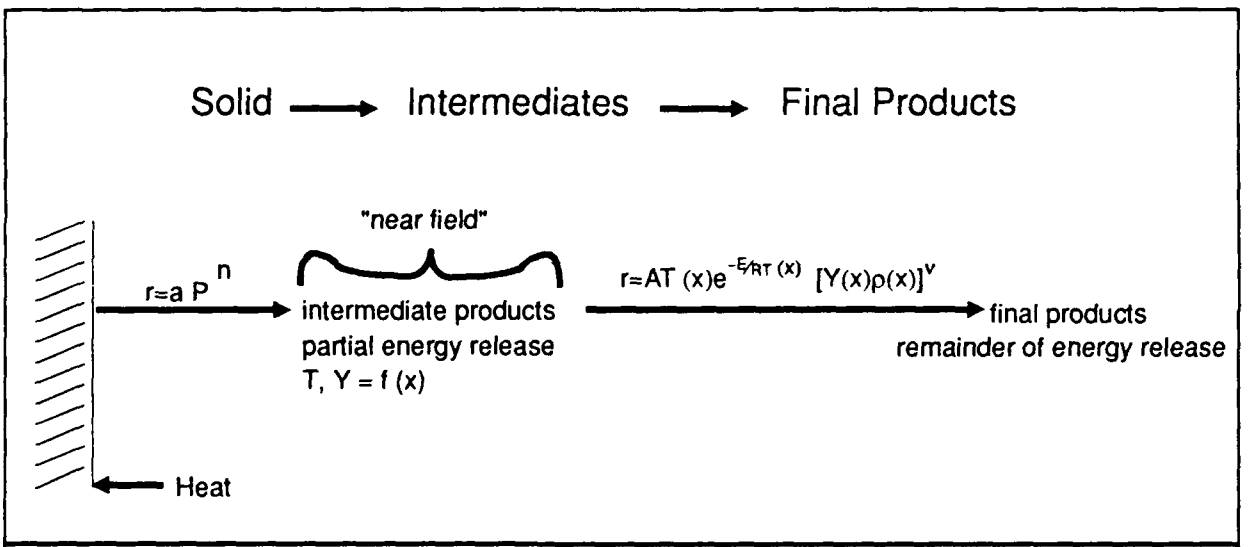

Figure 4. Schematic of Proposed Combustion Submodel

properties are those of the local macroscale, one may use the global kinetic data to determine in a natural manner the time-dependent composition and concomitant heat release of the intermediate products of combustion, as well as a consistent estimate of the heat feedback to the surface. The formulation of such a model will have to address a number of very difficult problems, including the effect of the crossflow, which is dominant during the ignition phase, and the positioning of the outer boundary of the local flame zone. However, it seems that these problems define one boundary of present day interior ballistic modeling and must be addressed if further progress is to be made not only in the theory of flamespreading but also perhaps in tube erosion.

B. The Effects of Propellant Grain Fracture

1. Background. The problem of ignition-induced pressure waves with subsequent grain fracture may be briefly reviewed as follows. The initial conditions within the gun are often such that the propellant does not fill all of the available volume in the chamber, either because the propellant may have settled (as for cased ammunition) or the charge package itself may be undersized with respect to the chamber (as for artillery charges). Further, the ignition system provides a local stimulus which leads to a nonuniform ignition of the main propellant charge. During the ensuing flamespreading, the interplay of several processes determines whether significant pressure waves are formed as well as their influence on the overall ballistic cycle.

Once ignition occurs at some point within the charge, there exists a competition between the local gas generation rates, determining the rate of local gas production and pressurization, and macroscopic charge permeability, determining the ease with which this local accumulation of gases can be transported to the rest of the gun chamber. The rate of gas generation is controlled by the intrinsic burning properties of the propellant as well as by its geometry, which influences both surface area and loading density. Macroscopic charge permeability includes contributions from both the configuration of the propellant and the distribution of free space, or ullage, within the chamber. (For example, the natural channels through a bundle of stick propellant offer much less resistance to gas flow than does the tortuous path through a bed of granular propellant.) Mobility of the charge itself may be important, as early dispersal of the propellant bed may both decrease local production rates and increase permeability. Unfortunately, subsequent impact of propellant grains against the chamber walls or projectile base can lead to local regions of high loading density and even propellant fracture, with attendant increases in burning surface.

Thus, at least two stages of the interior ballistic process have been identified where propellant fracture can occur: first, as a consequence of intergranular stresses resulting from the pressure gradient associated with either the primer blast itself or the progression of the convectively driven flame front through the bed; and second, as a direct result of impact against the projectile base or other chamber boundary, after having been accelerated by the pressure gradient and associated interphase drag forces.

Clearly, long bayonet primers, centercore igniters, and other distributed ignition systems all represent attempts to mitigate this situation. While such techniques often work well, their possible failure (e.g., separation of a primer flashtube from its headstock) may lead to serious problems. Further, many new projectiles, particularly for tank guns, protrude into the cartridge case, precluding the use of conventional, long bayonet primers. Coupled with the high propellant loading densities typifying modern tank ammunition, some level of longitudinal waves can be expected; depending on the mechanical properties of the propellant used, particularly at cold temperatures, the potential for catastrophe exists.

2. Modeling the Effects of Grain Fracture. Classical interior ballistics makes the implicit assumption of propellant grain incompressibility and nondeformability in treating the burning surface profile via a simple form function. Modern, multiphase flow pictures of the interior ballistic cycle recognize, however, the role of propellant bed rheology as

significant to the overall process. While individual grains are usually still treated as being incompressible, compaction of an aggregate of grains is allowed, with intergranular stresses in excess of ambient gas pressure typically taken to be dependent on bed porosity and perhaps its loading history. The scheme employed by the NOVA code[8] for about a decade now is depicted in Figure 5. Gough embeds his constitutive law into a formula for the rate of propagation of intergranular disturbances:

$$a(\varepsilon) = \left[-\frac{g_o}{\rho_p} \frac{d\sigma}{d\varepsilon} \right]^{\frac{1}{2}} ,$$

where $a(\varepsilon)$ = rate of propagation of intergranular disturbances

g_o = constant to reconcile units

ρ_p = density of the solid propellant

$\sigma = (1 - \varepsilon) R$,

R being the average stress due to contacts between particles and can be related to experimental data for loading and unloading according to the logic of Figure 5.

The current extensions to XNOVAKTC are two-fold. First, constitutive modeling has been extended to represent the influence of stress-induced grain fracture on surface area, affecting not only local mass generation rates but also interphase drag and heat transfer. Second, numerical analysis has been incorporated to treat the impact-induced compaction/stress wave as an explicit discontinuity, facilitating treatment of both sources of stress-induced grain fracture identified in the previous section.

It is then assumed that the extent of grain fracture can be represented as a local function of the maximum intergranular stress experienced throughout the propellant bed. As the solution develops, the maximum stress at each location is tracked, and the influence of any associated fracture is assumed to be characterized by a table of multipliers which depend on this maximum stress. Such data may be acquired by placing stressed samples of propellant in a closed bomb and then performing an inverse burning rate analysis in which a known burning rate allows determination of the surface profile. The multiplier is then simply expressed as the ratio of the actual area to that predicted by the form function for the unstressed propellant. The present version of the code does not include a

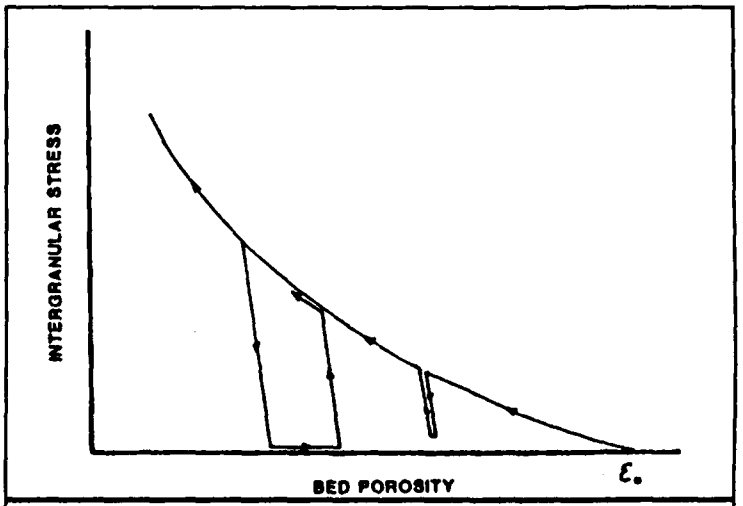

Figure 5. Schematic Depiction of Granular Stress Law Employed in NOVA Code

provision for the surface multiplier to be a function of fraction of the grain burned, but this feature could be easily added.

The latest XNOVAKTC code permits the stress history to alter not only the mass generation rate but also the interphase drag and heat transfer as they too relate to surface area. In some cases, however, it may be that increases in burning surface may result from embedded fractures that do not lead to total cleavage of the grains. Accordingly, the multipliers for interphase drag and heat transfer are not required to track those for the burning surface and may be specified independently.

3. Application. The extended XNOVAKTC code has been employed to study the possible effects of grain fracture in the 120-mm, M829 APFSDS kinetic energy tank round, depicted in Figure 6. The cartridge employs JA2 granular propellant as the main charge, ignited by a bayonet primer containing Benite strands as the ignition material. A major modeling complexity results from the presence of a combustible case; input data describing the burning properties of the case follow the earlier work of Robbins et al.[37] All standard input data are a result of independent measurements or reflect design dimensions. The resulting baseline data are included as Appendix B.

For this initial exercise, grain fracture data were obtained from studies reported by Lieb,[38] reflecting mini-closed bomb assessment of JA2 propellant grains damaged by firing in the Gas Gun Impact Tester.[39] Significant damage was noted for grains conditioned to temperatures of -20°C and below, particularly at impact velocities on the order of 100 m/s, for which surface area increases up to a factor of twelve were observed. These observations were not used directly in our simulations; rather, a table was constructed relating surface area multipliers to aggregate stress levels predicted by XNOVAKTC to be appropriate for the corresponding impact velocities.

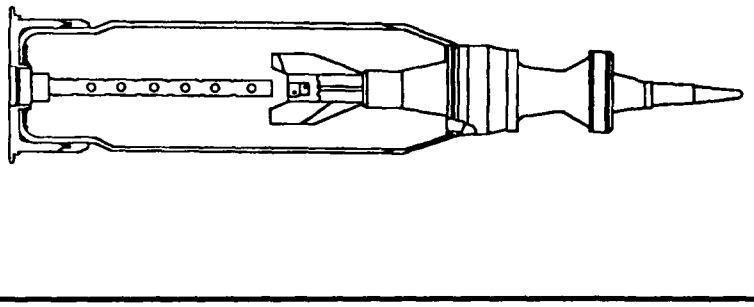

Figure 6. 120-mm, M829 Cartridge, APFSDS-T

The results of three calculations are reported here: first, a nominal run for a cold-conditioned (-25°C) XM829 round; second, a run including the effects of grain fracture as prescribed by Table 3 on an otherwise properly functioning round; and third, a simulation with localized base ignition (as might occur if a primer tube failed) and 25 mm of ullage at the front of the propellant bed (allowing for acceleration and impact of propellant grains -- clearly, an undesirable situation). Figures 7 through 9 display the predicted pressure-time and pressure-difference (breech minus forward chamber pressures) profiles for the three cases, clearly indicating the influence of the latter conditions. Figures 10 through 12 provide some additional insight into the phenomenology involved, displaying the intergranular stress profiles experienced by the propellant bed during flamespreading and early

propellant motion. As the convectively driven flame front passes through the bed, three different levels of interaction can be identified. As long as the stress level remains below the threshold value for fracture, no feedback exists from additional burning surface to further drive the pressure gradient and associated stress levels. Once fracture is initiated during the flamespreading process, however, an increase in the rate of stress growth may be expected, corresponding to the stronger local mass generation rates (and perhaps further exacerbated by a reduction in bed permeability). Finally, upon impact, significant increases in stress may result, with corresponding increases in fracture and substantial bootstrapping of the entire process.

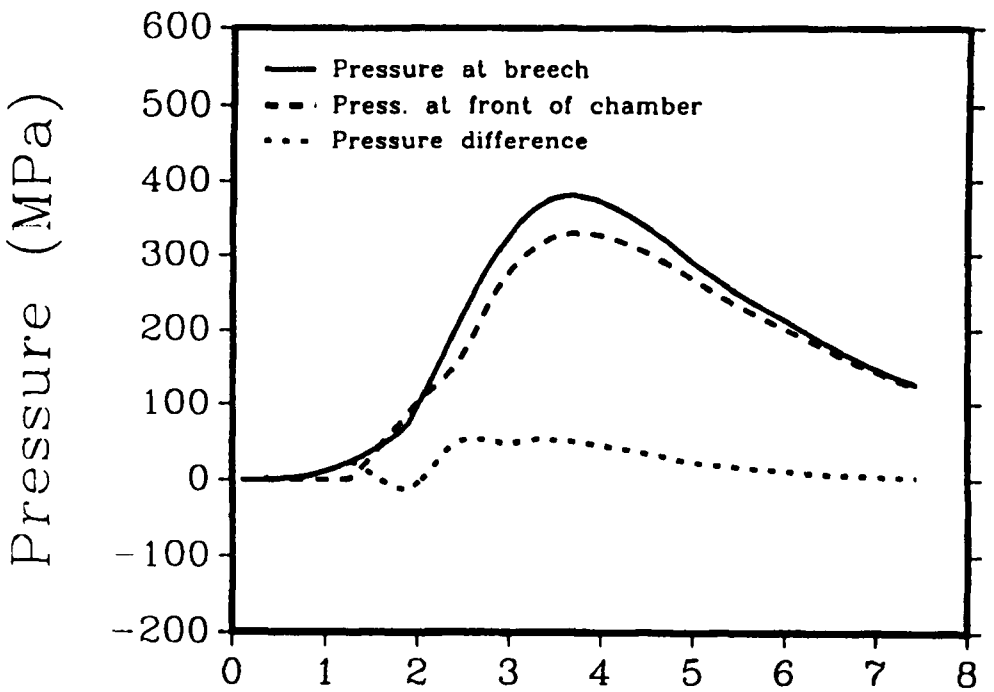

Figure 7. Predicted Pressure Profiles - Cold Baseline

The effects of grain fracture are very tightly interwoven into the overall ballistic process, so that the maximum stress levels shown in Figures 10 and 11 are less than those one might have expected. Interestingly, early stress-induced grain fracture at the front of the bed increases local pressurization and retards forward gas and grain velocities, the net result being a reduction in subsequent, bulk forward motion of the bed, mitigating the potential for further increases in local intergranular stress.

Table 3. Propellant Surface Area Multipliers

Stress (MPa)	0.0	10.0	25.0	50.0
Multiplier	1.0	1.0	2.0	10.0

The applicability of this new capability to the assessment of the interplay between ignition-induced pressure

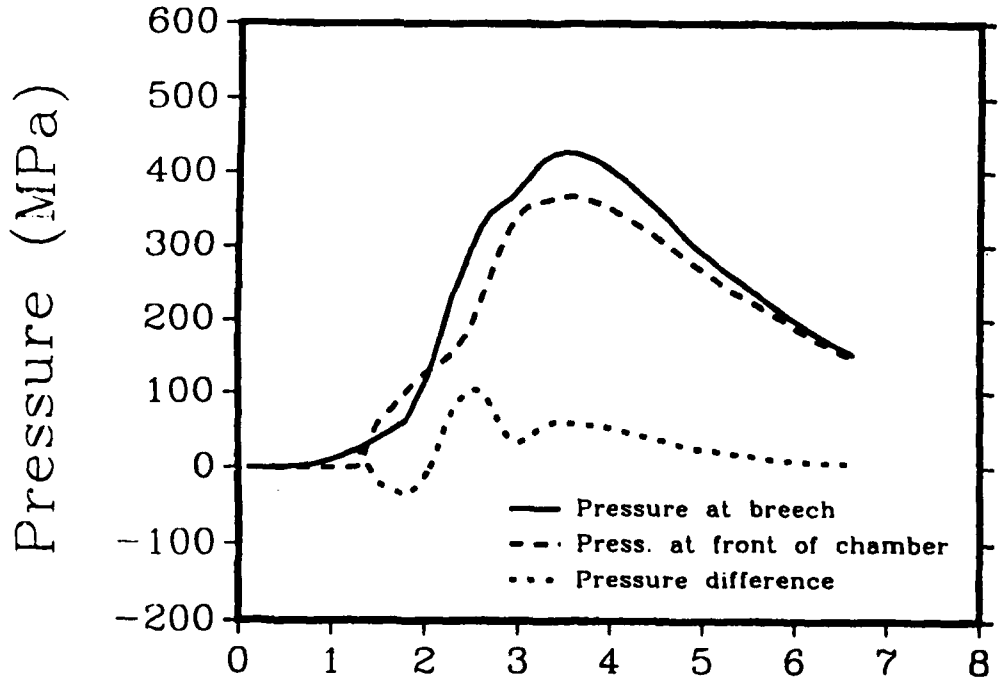

Figure 8. Predicted Pressure Profiles - Baseline Plus Grain Fracture

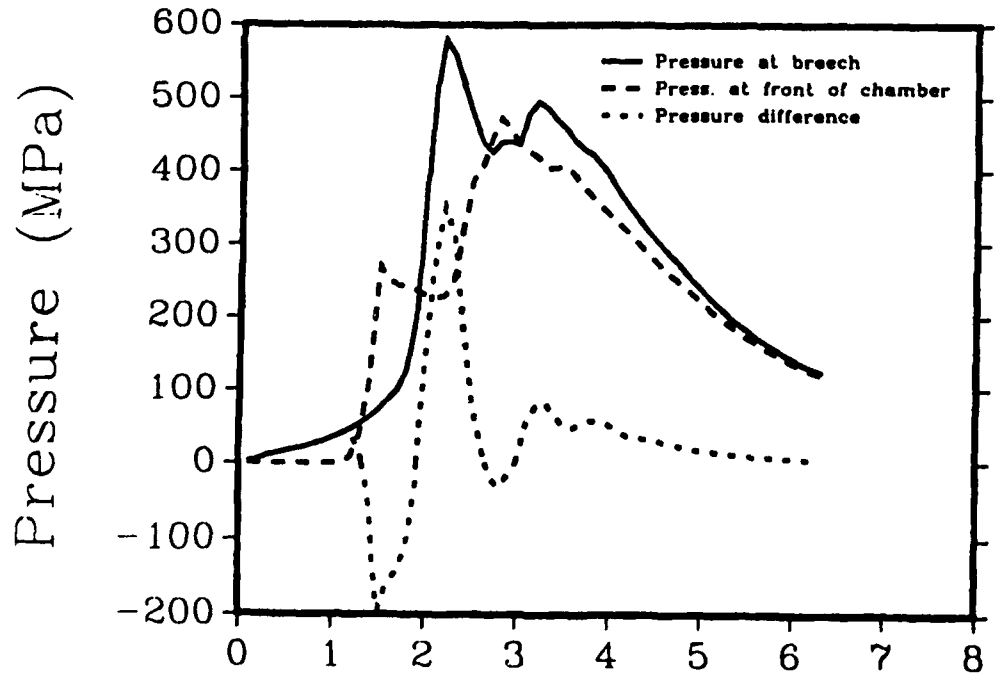

Figure 9. Predicted Pressure Profiles - Base Ignition, Forward Ullage, and Grain Fracture

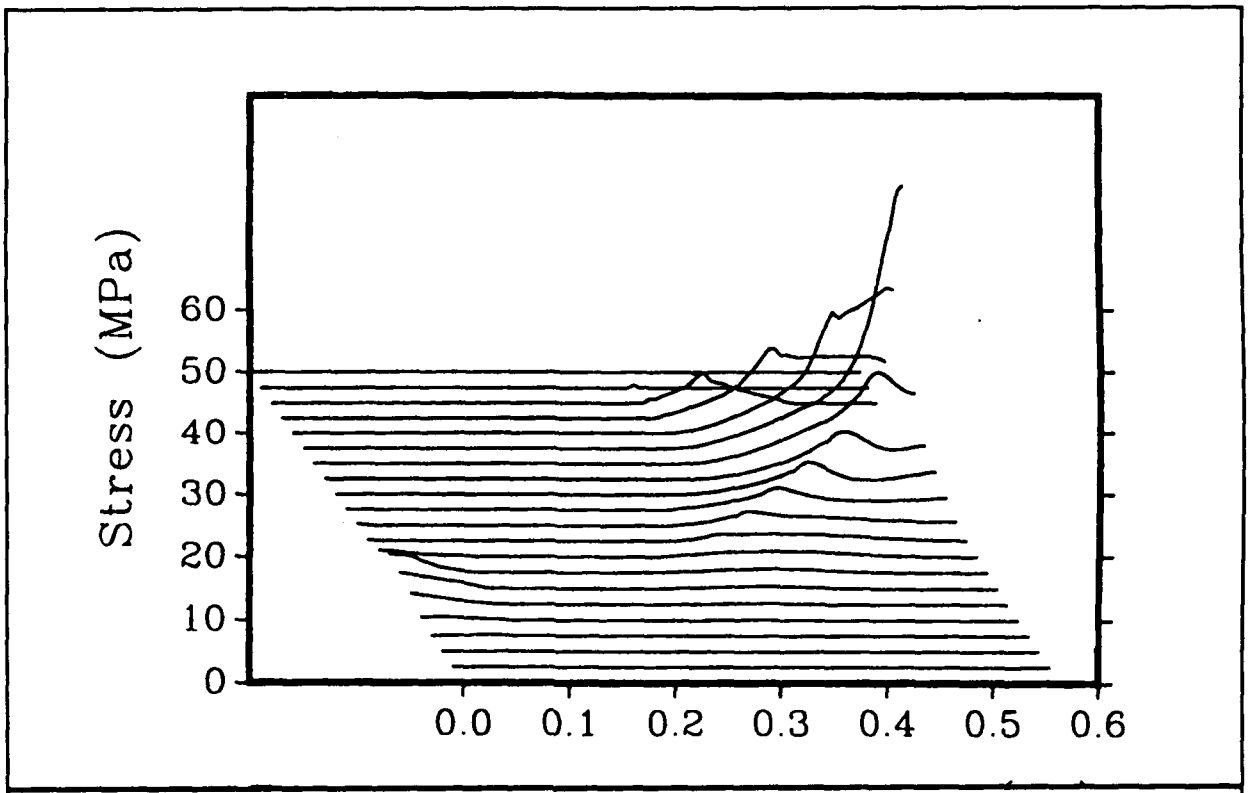

Figure 10. Progression of Intergranular Stress Profiles - Cold Baseline

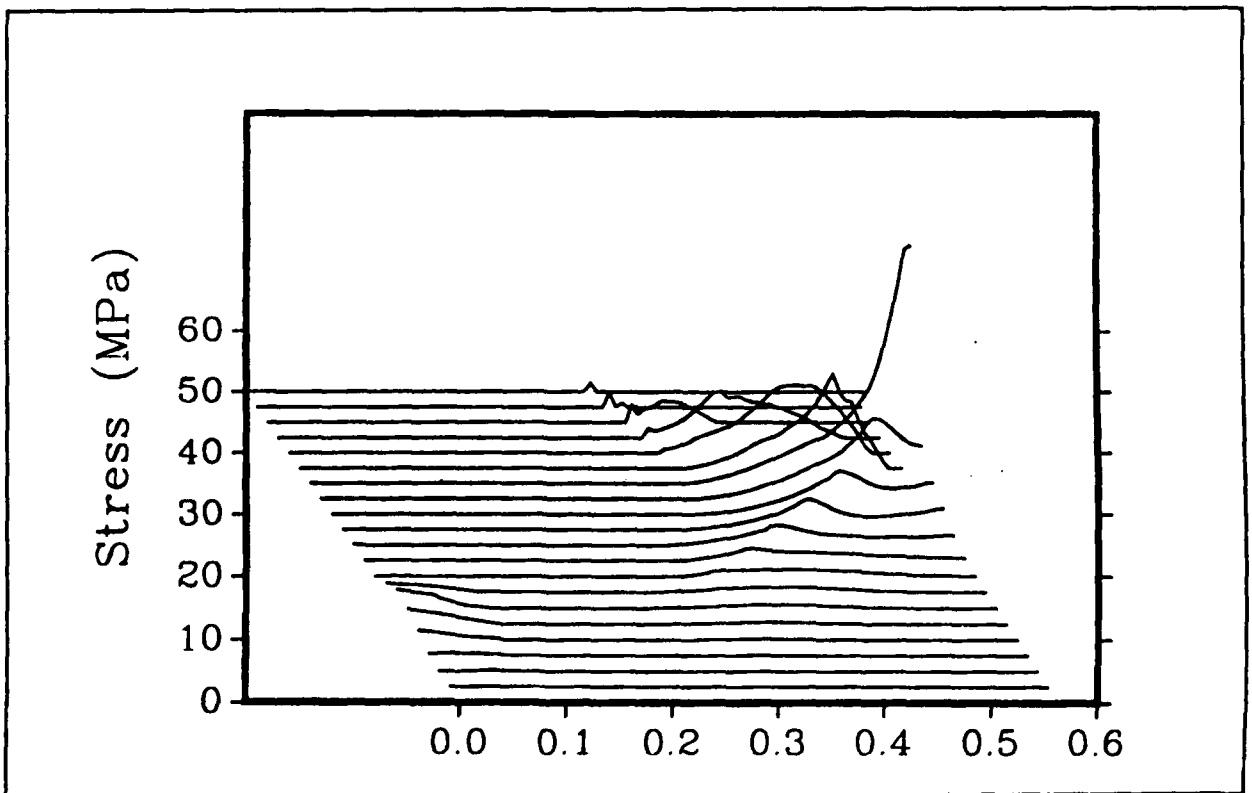

Figure 11. Progression of Intergranular Stress Profiles - Baseline Plus Grain Fracture

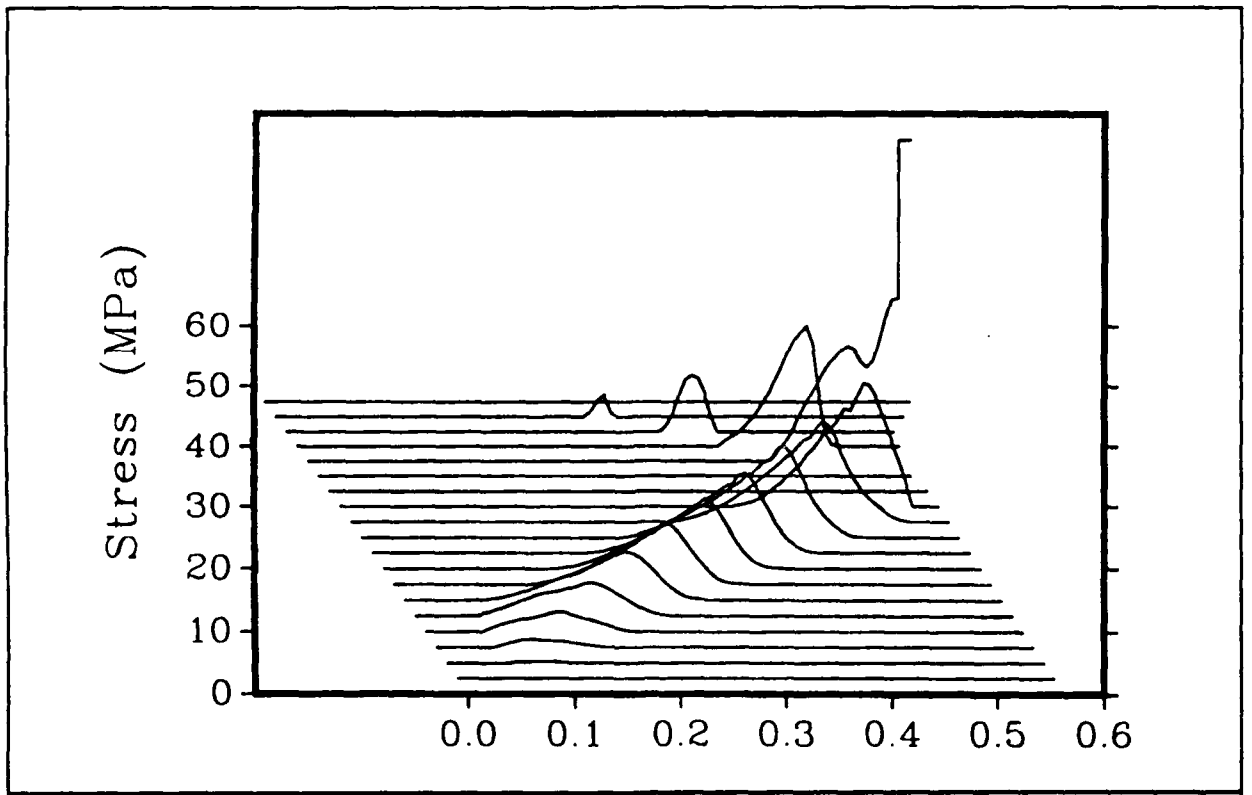

Figure 12. Progression of Intergranular Stress Profiles - Base Ignition, Forward Ullage, and Grain Fracture

waves and propellant mechanical properties offers a great improvement in terms of automation over previous effects to provide a descriptive and diagnostic evaluation capability with respect to breechblow phenomenology.[4,28,40]

4. Future Plans. An alternative technique for implementation of grain fracture into the XNOVAKTC represention involves use of a statistical distribution of fragment sizes to characterize the effective form functions for the particles.[41] These effective form functions can be quite complex, potentially including superimposed contributions from a variety of temperature and impact histories. Future work will also focus on a closer coordination between model formulation and experimental efforts to characterize both bed and individual grain response to intergranular stress waves as well as impact conditions.

C. Incorporation of Viscous Effects

1. Statement of the Problem. The problem of thermal erosion of gun tubes has received considerable attention from theoreticians over the years. The methods of investigation have ranged from the use of empirical heat transfer correlations[42] to the direct numerical solution of the two-dimensional, unsteady Navier-Stokes equations.[21-24,43] However, even in the most elaborate models reported to date, the details of ignition and packaging of the propelling charge have either been greatly simplified or ignored altogether. (Indeed, most of the solutions published have addressed the so-called Lagrange gun, in which a projectile is accelerated by a non-reacting gas which is initially at rest and high pressure.)

Yet, artillery charges are usually packaged in a container which may incorporate both combustible elements and additives intended to reduce bore erosion. The container is usually subcaliber with respect to the chamber, with the combustion and mechanical behavior of the case, as well as the presence of any annular ullage, likely to influence the formation of the tube wall boundary layer, including the introduction into it of any wear reducing additive materials.

Clearly, a complete theoretical treatment of the thermal erosion taking these features into account is a formidable task. Even if one adopts a macroscopic perspective in order to smooth out the structure associated with the granularity of the charge, the flow remains three-dimensional, as the charge is not loaded axisymmetrically. (Recent experimental data in 155-mm howitzers confirms the existence of highly asymmetic wear profiles.[44]) Then, too, the adoption of a macroscopic perspective for the sake of tractability introduces fundamental uncertainties, since the length scale of the wall boundary layer may be even smaller than that due to granularity of the charge. Further, it is not clear how one should represent the effects of turbulence in the highly transient gun environment, particularly if the presence of the burning propellant is to be taken into account. Additional physical uncertainties and complexities of bookkeeping are associated with the decomposition and dispersal of the container.

Current versions of both NOVA and TDNOVA incorporate the model of Shelton, et al.,[45] in which the development of the boundary layer is modeled according to a transient integral formulation; however, computational experience has shown it to be unsatisfactory for all but to the simplest charge configurations. The boundary layer displacement thickness is found to be susceptible to an unbounded growth mode which appears to be intrinsic to the model. Accordingly, an improved formulation is warranted.

2. Linkage of an Implicit Navier-Stokes Solver to TDNOVA to Form VTDNOVA. An appropriate extension to the existing heat transfer analysis of TDNOVA is embodied in the Navier-Stokes equations, with a retention of both the viscous stress and heat conduction terms. Such a formulation permits the automatic calculation of heat transfer to the tube in a manner which is intrinsically coupled to the development of the flow. However, the incorporation of the viscous and heat conduction terms into the basic formulation of TDNOVA raises a number of questions which range from the fundamental basis for the equations to the complex details of the method of numerical solution.

We have already alluded to several fundamental questions. These include a) the reconciliation of the macroscopic perspective, in terms of which the governing equations of TDNOVA are derived, with the microscopic length scales which characterize the structure of the boundary layer near the tube wall, b) the relevance of the Navier-Stokes representation of the diffusive terms in the gun environment, and c) the influence of the solid- phase on the structure of the turbulent flow. These questions are not answered at the present time. We make the working assumption that the Navier-Stokes equations can be applied to the region of ullage outside the propelling charge. The state of the gas-phase within the region occupied by the mixture continues to be represented in terms of the macroscopic or averaged equations which capture the viscid and thermal interactions between the gas and solid phases in terms of local algebraic correlations rather than as

diffusive processes (see Figure 13). The external and internal states are linked through the imposition of macroscopic jump conditions which are applied at the boundary of the mixture. Clearly, this approach presupposes the existence at all times of ullage between the charge and the tube wall. For some artillery charges circumferential ullage is clearly present, at least initially, within the framework of a two-dimensional axisymmetric representation. But, as the charge container ruptures, grains will be expected to move radially so that the circumferential ullage may eventually disappear. For tank charges, on the other hand, it is not obvious that circumferential ullage is ever present. We assume that this apparent disparity can be resolved by noting that ullage, as referred to in these comments on charge configuration, is in fact a macroscopic concept. We assume that the representation of the expansion of the charge to the tube wall can be accommodated in a way which is consistent with the length scales of both the interior mixture equations and the exterior boundary layer equations.

Previous TDNOVA calculations regarded contact with the wall as occurring when the normal spacing became less than 1 mm, a dimension small by comparison with the scale of heterogeneity of the mixture. On the other hand, evidence to date suggests that the thickness of the wall boundary layer may not be much larger than 1 mm. Thus, in a purely practical sense, it appears that this basic algorithm assumption can be satisfied. This discussion does not in any way address the much deeper questions which relate to the physical interpretation of the internal boundary conditions when expressed in terms of state variables which pertain to disparate length scales. We assume, as a working hypothesis, that the single-phase Navier-Stokes solution remains meaningful near the wall because the sensible intrusion of the solid propellant is limited by its lack of geometric conformality with the tube, and that the effects of the turbulent shear due to the boundary layers around the grains are captured, at least in part, by the imposition of the tangential momentum balance at the internal boundary.

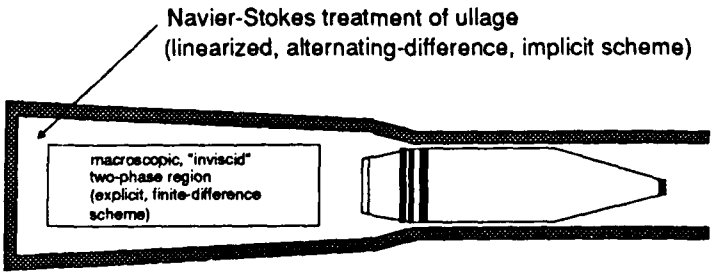

Figure 13. Schematic of the VTDNOVA Code

The extension of TDNOVA to incorporate viscous and heat transfer terms may be viewed as involving three separate steps. First, we note that the fully two-dimensional solution method of TDNOVA is normally continued only until the point at which the charge is ignited, the container has completely ruptured, and the radial pressure gradient has everywhere relaxed to a value less than a user-specified tolerance. The subsequent solution is normally completed using a quasi-two-dimensional representation of the charge. This approach, originally adopted for reasons of computational economy, has the effect of avoiding to a large degree the possibility of instability of the boundary of the mixture. An aggregate of dispersed propellant grains has a natural physical tendency to assume unbounded distortions of its boundaries. If such distortions arise, the finite difference method of solution can be destabilized by the inability of the mesh to capture increasing amounts of geometrical data. Coupling between the numerical and physical modes of instability can result in a rapid loss of accuracy or even in total breakdown of the solution. This difficult topic is part of a longer range investigation as discussed in the next section. For the time being, it has been determined that stabilization of the boundaries of the propellant using artificial means permits fully two-dimensional solutions to be continued to the point at which the projectile exits the gun. Studies are in progress to determine the minimum necessary degree of stabilization of the boundaries.

The second step involves the development of a means of solution of the Navier-Stokes equations in a manner which is compatible with the pre-existing TDNOVA formulation insofar as the analysis of boundary values is concerned. The particular form of the equations is described elsewhere.[16] The method of solution employed is similar to that of Schmitt[21] and is based on a Linearized Alternating Direction Implicit Algorithm. The resulting computational module, known as LADIS, has been linked to a special version of TDNOVA to produce a code called TDLADIS whose applicability is restricted to single-phase flow. TDLADIS was first exercised by reference to the Lagrange ballistic problem for which an analytical solution was obtained by Love and Pidduck.[46] This is the same problem that previous investigators have used to validate the TDNOVA,[47] ALPHA,[48] and DELTA[21] codes.

This problem has been fully described by these previous investigators and requires no particular discussion here. We are given a quiescent pressurized gas which propels a projectile through a cylindrical, frictionless tube. The results are reported in detail in the reference;[16] suffice it to say here that although the accuracy of the implicit scheme is shown to be not as good as that of TDNOVA, which is specifically oriented towards wave propagation problems, the agreement between TDLADIS and the analytical results is certainly acceptable. Moreover, the accuracy appears to be at least as good as that reported for the DELTA code[21] and better than that reported for the ALPHA code.[48] Global mass balancing was quite satisfactory; the final and extremal value of disparity was 0.22%. Further, calculated breech pressures never differed by more than 0.58% from the analytical solution, projectile base pressures never by more than 0.71%.

More recent work has focused the problem first studied by Heiser and Hensel[22] and subsequently by Schmitt and Mann.[48] We are again concerned with a Lagrange type of ballistic problem but the flow is taken to be viscid and heat conducting. Details of the data base may be found in reference 48. Solutions obtained with TDLADIS appear to be in

agreement with those obtained with the ALPHA code in several respects, including values of muzzle velocity, final boundary layer thickness, and details of the radial flow field. Present work with TDLADIS is confined to a study of the effects of alternative formulations of the boundary value analysis on the details of the solution near the corners. Particular interest is given to the singular condition at the intersection of the tube wall and the base of the projectile.

The third step involves the linkage of LADIS to TDNOVA to produce a code referred to as VTDNOVA, the ultimate goal of the present study. At the present time the details of the necessary coding linkages have been worked out, but testing and debugging will be performed only when the final choice of boundary value analysis for LADIS is complete.

III. FUTURE EFFORTS: A NEXT GENERATION MODEL

The VTDNOVA code is expected to permit an assessment of the influence of charge packaging and ignition on the development of the thermal boundary layer at the tube wall. While the code is expected to provide new theoretical insights into the problem of thermal erosion, it must be admitted that it will leave many questions unanswered. We have already noted certain fundamental problems which will require attention: reconciliation of length scales; instability of the mixture boundary; turbulence laws. Apart from these, one may observe that thermal erosion of artillery weapons is not axisymmetrical so that a three-dimensional representation is really required. VTDNOVA treats the charge container, whether bag or combustible case, as an attribute of the mixture boundary; an extension is required to represent the breakup and dispersal of the container, particularly when wear-reducing additives are present.

A next generation model will clearly be based on a three-dimensional formulation, not only for studies of heat transfer but also for certain problems of flamespreading and of the computation of the loads on the afterbody of a finned projectile. However, much more is required than a simple integration of the three-dimensional equations for multiphase flow. Our experience with the development of the NOVA and TDNOVA codes has convinced us of the importance of relatively fine details of the macroscopic geometry. NOVA and TDNOVA pay close attention to the distribution of ullage and TDNOVA incorporates properties of the container into the boundary conditions for the mixture. As we have extended our continuum studies, the importance of fine geometric details has likewise increased. We expect this trend to continue when we turn to a three-dimensional formulation. We may also draw from past experience and note that continuum modeling per se does not add much to the analysis of nominal ballistic behavior. As may be seen from the previous discussion of chemistry and grain fracture, the conditions under which charges behave anomalously always seem to involve an interplay between continuum response and shifts in constitutive behavior. It seems that a next generation model must permit the inclusion those details of chemistry and grain fracture which have been considered in the NOVA code. Finally, in respect to the scope of the model, we should note that many modern charges, particularly those designed for tank weapons, include several packages of propellant which may be arranged so as to create complex internal boundaries.

It is evident that the development of the next generation model will be an ambitious undertaking. Because of the scope of the undertaking we intend to reappraise many basic aspects of interior ballistic modeling. Rather than proceeding directly to extend VTDNOVA to a third dimension, we plan to consider whether alternative approaches might offer potential advantages. The following remarks are intended to sketch the areas of interest.

First, we intend to give consideration to the trends in computer technology. When the NOVA code was first written, some fifteen years ago, code size and computation time were serious concerns. Today, complete calculations can be made on the CRAY computer in less than 10 seconds. In fact, there are versions of NOVA, which are far more complex than the original version, which run on desktop computers like the IBM PC-AT. Taking into account the development time of a next generation code and assuming longevity comparable to that of NOVA, it seems prudent to assume that the new code will enjoy hardware advances which will be made over the next ten to twenty years. However, the ramifications of hardware advances go beyond considerations of machine size and speed, factors which constrain the level of detail of modeling. One must also consider the probability of significant changes in architecture. We have already seen the advent of parallel processing as an alternative to older designs. There is some discussion of the possibility that massively parallel systems will become available for hydrodynamic simulations. Such a possibility would impact on the choice of solution algorithm for a new code. Implicit schemes might not retain sufficient computational advantage to justify their use in place of the simpler, and more easily maintainable explicit schemes.

It will also be necessary to reconsider the overall representation of the flow, both from a fundamental and from a computational perspective. The current representation of VTDNOVA is predicated on the equations of macroscopic two-phase flow. Both phases are viewed as continua and the boundaries of each mixture region are viewed as macroscopic discontinuities across which the porosity and all the other averaged state variables may experience finite jumps in value. These internal boundaries are tracked explicitly as part of the solution technique and are responsible for the creation of a great deal of administrative coding. We have already commented on difficulties created by the possibility of unstable motion of the boundaries. A second difficulty relates to the behavior of the gas phase when it crosses an internal boundary. Strictly speaking, the balance of tangential momentum requires that the transverse component of velocity be conserved. However, from the macroscopic perspective it appears that a relaxation zone will be present for entering gas and that this zone will be so small as to justify the representation of a tangential momentum loss within the finite jump conditions. Such an approach was found to be necessary in order to obtain stable solutions in the TDNOVA code. Alternative representations might be found among the following possibilities.

One possibility would be to treat only the products of combustion as a continuum. For a three-dimensional simulation with a 20x20x20 mesh, a total of 8000 points would be required. This number is comparable to the total number of grains in the charge. Accordingly it becomes practical to consider following the motion of each and every grain, viewed as a rigid body or possibly with a few degrees of distortional freedom. Rather than a continuum-oriented intergranular stress field, one would consider directly the forces between grains. The porosity could be computed by explicit averaging over the instan-

taneous configuration of the aggregate. The gas-phase equations would be extended to reflect additional correlation terms arising from the averaging process supported by simple models of the microstructure. A finite difference mesh would be required to model only the state of the gas phase, and this mesh could be made adaptive to the strong gradients of porosity at the mixture boundaries. Arbitrary numbers of packages would be handled automatically without undue bookkeeping burdens. The containers would be treated according to the same procedure as the propellant grains and would move independently of the mixture boundaries. Fracture of the container, as well as of individual grains, would be easily represented. The ambiguities associated with the analysis of mixture boundaries would be largely circumvented. Obviously, such a representation would require a great deal of storage, and the analysis of its feasibility would have to take into account the expected trends in computer hardware discussed in the previous paragraph.

Certain other topics are thought to warrant further investigation. Among these we may mention here the possibility that ensemble averaging may provide a way of reconciling the length scale of the wall boundary layer with the macroscopic state variables used to model the mixture. Also, it may of value to pursue a formulation in which the state of the boundary layer is viewed as an attribute of the local fluctuation field, which is then modeled as co-existing with the macroscopic field rather than being linked through a boundary condition.

As a closing comment we should note that the development of a next generation code is expected to have ramifications for the lower order models. The development of TDNOVA led to improved numerical procedures which in turn were incorporated in NOVA to produce a smaller, faster and more maintainable code. The insights into flow structure provided by the NOVA solutions permitted the development of more sophisticated analyses of the pressure gradient as required by the lumped- parameter interior ballistic codes.

REFERENCES

1. P.G. Baer and J.M. Frankle, "The Simulation of Interior Ballistic Performance of Guns by Digital Computer Program," BRL Report No. 1183, USA ARDC, Ballistic Research Laboratories, Aberdeen Proving Ground, MD, December 1962.

2. K.D. Fickie and J. Grosh, "A Technique for Code Augmentation," BRL-MR-3622, US Army Ballistic Research Laboratory, Aberdeen Proving Ground, MD, October 1987.

3. A.J. Budka and J.D. Knapton, "Pressure Wave Generation in Gun Systems: A Survey," BRL-MR-2567, USA Ballistic Research Laboratories, Aberdeen Proving Ground, MD, December 1975.

4. I.W. May and A.W. Horst, "Charge Design Considerations and Their Effect on Pressure Waves in Guns," ARBRL-TR-02277, USA ARRADCOM, Ballistic Research Laboratory, Aberdeen Proving Ground, MD, December 1980.

5. E.B. Fisher, "Continued Development and Documentation of the Calspan Interior Ballistics Code," Calspan Report No. 6689-D-1, Calspan Corporation, Buffalo, NY, February 1981.

6. P.S. Gough, "The Flow of a Compressible Gas Through an Aggregate of Mobile Reacting Particles," IHCR 80-7, Naval Ordnance Station, Indian Head, MD, December 1980.

7. K.K. Kuo and J.H. Koo, "Transient Combustion in Granular Propellant Beds. Part I: Theoretical Modeling and Numerical Solution of Transient Combustion Processes in Mobile Granular Propellant Beds," BRL-CR-346, USA ARRADCOM, Ballistic Research Laboratory, Aberdeen Proving Ground, MD, August 1977.

8. P.S. Gough, "The NOVA Code: A User's Manual. Volume 1. Description and Use," IHCR 80-8, Naval Ordnance Station, Indian Head, MD, December 1980.

9. A.W. Horst, C.W. Nelson, and I.W. May, "Flame Spreading in Granular Propellant Beds: A Diagnostic Comparison of Theory to Experiment," AIAA Paper No. 77-856, AIAA/SAE 13th Propulsion Conference, Orlando, FL, July 1977.

10. A.W. Horst and P.S. Gough, "Influence of Propellant Packaging on Performance of Navy Case Gun Ammunition," Journal of Ballistics, Vol. 1, No. 3, pp. 229-258, 1977.

11. E.B. Fisher and A.P. Trippe, "Development of a Basis for Acceptance of Continuously Produced Propellant," Calspan Report No. VQ-5163-D-1, Calspan Corporation, Buffalo, NY, November 1973.

12. P.S. Gough, "Theoretical Study of Two-Phase Flow Associated with Granular Bag Charges," ARBRL-CR-00381, USA ARRADCOM, Ballistic Research Laboratory, Aberdeen Proving Ground, MD, September 1978.

13. P.S. Gough, "A Two-Dimensional Model of the Interior Ballistics of Bagged Artillery Charges," ARBRL-CR-00452, USA ARRADCOM, Ballistic Research Laboratory, Aberdeen Proving Ground, MD, April 1981.

14. P.S. Gough, "Two-Dimensional, Two-Phase Modeling of Multi-Increment Bagged Artillery Charges," ARBRL-DR-00503, USA ARRADCOM, Ballistic Research Laboratory, Aberdeen Proving Ground, MD, February 1983.

15. P.S. Gough, "Modeling of Rigidized Gun Propelling Charges," ARBRL-CR-00518, USA ARRADCOM, Ballistic Research Laboratory, Aberdeen Proving Ground, MD, November 1983.

16. P.S. Gough, "Numerical Simulation of Current Artillery Charges Using the TDNOVA Code," BRL-CR-555, US Army Ballistic Research Laboratory, Aberdeen Proving Ground, MD, June 1986.

17. A.W. Horst, F.W. Robbins, and P.S. Gough, "A Two-Dimensional, Two-Phase Flow Simulation of Ignition, Flamespread, and Pressure-Wave Phenomena in the 155-mm Howitzer," ARBRL-TR-02414, USA ARRADCOM, Ballistic Research Laboratory, Aberdeen Proving Ground, MD, July 1982.

18. A.W. Horst, F.W. Robbins, and P.S. Gough, "Multidimensional, Multiphase Flow Analysis of Flamespreading in a Stick Propellant Charge," ARBRL-MR-03372, USA ARRADCOM, Ballistic Research Laboratory, Aberdeen Proving Ground, MD, August, 1984.

19. P.S. Gough, "XNOVAT. A Two-Phase Flow Model of Tank Gun Interior Ballistics," PGA-TR-85-2, Paul Gough Associates, Portsmouth, NH, October 1985.

20. P.S. Gough, "The XNOVAKTC Code," PGA-TR-86-1, Paul Gough Associates, Portsmouth, NH, March 1986.

21. J.A. Schmitt, "A Numerical Algorithm for the Multidimensional, Multiphase Viscous Equations of Interior Ballistics," BRL-TR-2828, US Army Ballistic Research Laboratory, Aberdeen Proving Ground, MD, July 1987.

22. R. Heiser and D. Hensel, "Calculation of the Axisymmetric Unsteady Compressible Boundary Layer Flow Behind a Moving Projectile," Proceedings of the Fourth International Symposium on Ballistics, Naval Postgraduate School, Monterey, CA, 17-19 October 1978.

23. H.J. Gibeling and H. McDonald, "An Implicit Numerical Analysis for Two-Dimensional Turbulent Interior Ballistic Flows," BRL-CR-00523, USA ARDC, Ballistic Research Laboratory, Aberdeen Proving Ground, MD, February 1984.

24. A.C. Buckingham, "Dusty Gas Influences on Transport in Turbulent Erosive Propellant Flows," AIAA Journal, Vol. 19, p. 501, 1981.

25. J. Ludwig, N. Rhoades, and D.G. Tatchell, "Numerical Modelling of the Flow of a Hot Particle-Laden Gas," Proceedings of the Seventh International Symposium on Ballistics, The Hague, The Netherlands, pp. 37-51, April 1983.

26. Kolkert, W.J., Waas, M., and The, H.G., "On the Thermal Behavior of the Barrel during the Interior Ballistic Cycle of Propellant Guns," Proceedings of the Propulsion and Energetics Panel of the NATO Advisory Group for Aerospace Research and Development, 66th B Specialists Meeting on the Interior Ballistics of Guns, Florence, Italy, 9-11 September 1985.

27. T.C. Minor, "Characterization of Ignition Systems for Bagged Artillery Charges," ARBRL-TR-02377, USA ARRADCOM, Ballistic Research Laboratory, Aberdeen Proving Ground, MD, October 1981.

28. A.W. Horst, I.W. May, and E.V. Clarke, Jr., "The Missing Link Between Pressure Waves and Breechblows," ARBRL-MR-02849, USA ARRADCOM, Ballistic Research Laboratory, Aberdeen Proving Ground, MD, July 1978.

29. A.W. Horst, "Multiphase Flow Analysis of the Ballistic Performance of an Anomalous LOVA Propellant Mix," ARBRL-MR-03277, USA ARRADCOM, Ballistic Research Laboratory, Aberdeen Proving Ground, MD, June 1983.

30. G.E. Keller and A.W. Horst, "The Two Phase Flow Simulation of LOVA Propellant Interior Ballistic Behavior Using the XNOVAK Code, BRL-TR-2796, US Army Ballistic Research Laboratory, Aberdeen Proving Ground, MD, April 1987.

31. C.F. Price, personal communication.

32. M.W. Beckstead, N.L. Peterson, D.T. Pilcher, B.D. Hopkins, and H. Krier, "Convective Combustion Modeling Applied to Deflagration-to-Detonation Transition of HMX," Combustion and Flame, Vol. 30, pp. 231-241, 1977.

33. T.L. Boggs, C.F. Price, A.I. Atwood, D.E. Zurn, and R.L. Derr, "Role of Gas Phase Reactions in Deflagration-to-Detonation Transition," Seventh Symposium (International) on Detonation, Naval Weapons Center, NSWC MP-82-334, pp. 216-224, June 1981.

34. T.L Boggs, C.F. Price, and R.L Derr, "Transient Combustion: An Important Consideration in Deflagration-to-Detonation Transition," NATO Advisory Group for Aerospace Research and Development, Neuilly sur Seine, France, AGARD-CCP-367, pp. 12-1 to 12-20, May 1984.

35. C.F. Price and T.L Boggs, "Modeling the Deflagration-to-Detonation in Porous Beds of Propellant," Eighth Symposium (International) on Detonation, Vol. II, pp. 650-657, July 1985.

36. M. Summerfield, L.H. Caveny, R.A. Battista, N. Kubota, Gostintsev, A. Yu, and H. Isoda, "Theory of Dynamic Extinguishment of Solid Propellants with Special Reference to

Non-Steady Heat Feedback Law," Journal of Spacecraft and Rockets, Vol. 8, No. 3, 1971.

37. F.W. Robbins, A.A. Koszoru, and T.C. Minor, "A Theoretical and Experimental Interior Ballistic Characterization of Combustible Cases," Proceedings of the Ninth International Symposium on Ballistics, Royal Military College of Science, Shrivenham, Eng land, pp. 1-21 to 1-28, 29 April-1 May 1986.

38. R.J. Lieb, "Impact Generated Surface Area in Gun Propellants," BRL-TR-2946, USA LABCOM, Ballistic Research Laboratory, Aberdeen Proving Ground, MD, November 1988.

39. R.J. Lieb and J.J. Rocchio, "A Gas Gun Impact Tester for Solid Gun Propellants," BRL-MR-2946, US Army Ballistic Research Laboratory, Aberdeen Proving Ground, MD, October 1984.

40. A.W. Horst, "Breechblow Phenomenology Revisited," BRL-TR- 2707, US Army Ballistic Research Laboratory, Aberdeen Proving Ground, MD, January 1986.

41. E.B. Fisher, personal communication.

42. J. Corner, Theory of Interior Ballistics of Guns, John Wiley and Sons, Inc., New York, 1950.

43. R. Heiser and J.A. Schmitt, "Simulations of Special Interior Ballistic Phenomena With and Without Heat Transfer to the Gun Tube Wall," BRL-TR-2732, US Army Ballistic Research Laboratory, Aberdeen Proving Ground, MD, May 1986.

44. D.L. Kruczynski and I.C. Stobie, "Charge/Projectile/Gun Tube Interactions and Gun Tube Wear," BRL-TR-3004, USA LABCOM, Ballistic Research Laboratory, Aberdeen Proving Ground, MD, January 1989.

45. S. Shelton, A. Bergles, and P. Saha, "Study of Heat Transfer in Gun Barrels," AFATL-TR-73-69, Air Force Armament Laboratory, Eglin Air Force Base, FL, March 1973.

46. A.E.A. Love and F.B. Pidduck, "Lagrange Ballistic Problem," Phil. Trans. Roy. Soc., Vol. 222, pp. 167-226, 1921-2.

47. F.W. Robbins, "Comparison of TDNOVA Results with an Analytic Solution," ARBRL-MR-03299, USA ARRADCOM, Ballistic Research Laboratory, Aberdeen Proving Ground, MD, July 1983.

48. J.A. Schmitt and T.L. Mann, "An Evaluation of the ALPHA Code in its One-Phase Mode," ARBRL-MR-03081, USA ARRADCOM, Ballistic Research Laboratory, Aberdeen Proving Ground, MD, April 1981.

Appendix A

XNOVAKTC Input Data for 105-mm Tank Gun Firing LOVA Propellant

INTENTIONALLY LEFT BLANK.

XNOVAKTC: INPUT FILE CARD IMAGE

```
LOVA XM39 LOTA2-202 M489 PROJECTILE, TWO GAS PHASE REACTIONS
TFFFTTT          1      01
   17 3500    0 3500          .0001
0.05       188.       .0001     2.        .05       .01       .0002     .0001
    6    2    2    4    0    0    1    3    0    0    0    2

500.       14.7       29.       1.4
500.
LOVA XM39 LOTA2-202 0.         21.622     13.350    .05845
    9  .306     .015      .340      19.
17400.     .5        50000.              .5
6000.      .00006457 1.109     20000.    .006682   .5757     100000.   .0000203
1.161      0.        858.      .0277     .0001345  .6
15250000. 21.169     1.28120   28.44
9997000.  29.82       1.2254   16.78
0.         .004
3.         11.
4.41       4.41
0.         0.
0.         2.00      3.00      2.50      18.50     2.41      21.50     2.097
24.90      2.097     210.5     2.097
21.622     100.      22.622    2000.     24.5      500.      210.5     500.
21.622     23.2      44.       9.9
0.         21.622
    5    2    0
LOVA-I     G 3498.   4481.     28.64     20.954    0.0       0.0
BENITE     G 2867.5  3513.8    23.23     29.82     0.0       0.0
BENITE     S 2867.5  2867.5    0.0       0.0       0.06      .000
AIR        G 1604.89 2246.85   26.68     28.896    0.0       0.0
LOVA-F     G 3498.   4481.     28.64     20.954    0.0       0.0
 7625000. 1.0        0.0       0.0       0.0
9997373.  0.0        1.0       0.0       0.0
882690.   0.0        0.0       0.0       1.0
    1    0    0    0    5    0    0    0
1.0        0.0       0.0       0.0       1.0       0.0       0.0       0.0
7625000.   .145319E8 0.0       3.0E08    1.0       0.0       0.0
1.0
    1    2    0    0    5    2    0    0
1.0        1.0       0.0       0.0       1.0       1.0       0.0       0.0
7625000.   .145319E100.0       3.0E08    1.0       1.0       0.0
0.0
```

LOVA XM39 LOTA2-202 M489 PROJECTILE, TWO GAS PHASE REACTIONS

XNOVAKTC VERSION NUMBER 1.022

CONTROL DATA

LOGICAL VARIABLES:

PRINT T PLOT F DISK WRITE F DISK READ F

I.B. TABLE T FLAME TABLE T PRESSURE TABLE(S) T

```
EROSIVE EFFECT 0      WALL TEMPERATURE CALCULATION 0
BED PRECOMPRESSED 0
HEAT LOSS CALCULATION 0

BORE RESISTANCE FUNCTION 1
 1: LINEAR INTERPOLATION OF ENGRAVING RESISTANCE DATA
 2: LIKE 1 TIMES EXPONENTIAL VELOCITY FUNCTION
 3: LIKE 1 TIMES RATIONAL VELOCITY FUNCTION
 4: LIKE 1 PLUS AIR SHOCK
 5: LIKE 1 PLUS PROJECTILE SETBACK
 6: LIKE 1 PLUS AIR SHOCK AND PROJECTILE SETBACK

SOLID TRAVELING CHARGE OPTION (0=NO,1=YES)   0
EXPLICIT COMPACTION WAVE(0=NO;1=YES)   0
CONSERVATIVE SCHEME TO INTEGRATE SOLID-PHASE CONTINUITY EQUATION  (0=NO,OLD; 1=YES,NEW) 0
KINETICS MODE (0=NONE;1=GAS-PHASE ONLY;2=BOTH PHASES)   1
TANK GUN OPTION (0=NO,1=YES)    0
INPUT ECHO OPTION  0
FORWARD BOUNDARY CONDITION (0=CLOSED;1=OPEN;2=ROCKET)   0
LIQUID TRAVELING CHARGE OPTION(0=NO,1=YES)              0
GRAIN FRACTURE OPTION(0=NO;1=YES)                       0
GRAIN FRACTURE DATA BASED ON INTRINSIC AVERAGE STRESS
                              (0=NO;1=YES)              0
ELECTROTHERMAL GUN OPTION(0=NO;1=YES)                   0


                    INTEGRATION PARAMETERS
NUMBER OF STATIONS AT WHICH DATA ARE STORED          17
NUMBER OF STEPS BEFORE LOGOUT                      3500
TIME STEP FOR DISK START                              0
NUMBER OF STEPS FOR TERMINATION                    3500
TIME INTERVAL BEFORE LOGOUT(SEC)                0.1000E-03
TIME FOR TERMINATION (SEC)                      0.5000E-01
PROJECTILE TRAVEL FOR TERMINATION (INS)            188.00
MAXIMUM TIME STEP (SEC)                         0.1000E-03
STABILITY SAFETY FACTOR                              2.00
SOURCE STABILITY FACTOR                            0.0500
SPATIAL RESOLUTION FACTOR                          0.0100
TIME INTERVAL FOR I.B. TABLE STORAGE(SEC)       0.2000E-03
TIME INTERVAL FOR PRESSURE TABLE STORAGE (SEC)  0.1000E-03


                      FILE COUNTERS
NUMBER OF STATIONS TO SPECIFY TUBE RADIUS            6
NUMBER OF TIMES TO SPECIFY PRIMER DISCHARGE          2
NUMBER OF POSITIONS TO SPECIFY PRIMER DISCHARGE      2
NUMBER OF ENTRIES IN BORE RESISTANCE TABLE           4
NUMBER OF ENTRIES IN WALL TEMPERATURE TABLE          0
NUMBER OF ENTRIES IN FORWARD FILLER ELEMENT TABLE    0
NUMBER OF TYPES OF PROPELLANTS                       1
NUMBER OF BURN RATE DATA SETS                        3
NUMBER OF ENTRIES IN VOID FRACTION TABLE(S)          0    0    0
NUMBER OF ENTRIES IN PRESSURE HISTORY TABLES         2
NUMBER OF ENTRIES IN REAR FILLER ELEMENT TABLE       0
```

GENERAL PROPERTIES OF INITIAL AMBIENT GAS

INITIAL TEMPERATURE (DEG.R)	500.0
INITIAL PRESSURE (PSI)	14.7
MOLECULAR WEIGHT (LBM/LBMOL)	29.000
RATIO OF SPECIFIC HEATS	1.4000

GENERAL PROPERTIES OF PROPELLANT BED

INITIAL TEMPERATURE (DEG.R)	500.0
MINIMUM IMPACT VELOCITY FOR EXPLICIT COMPACTION WAVE (IN/SEC)	100000000.

PROPERTIES OF PROPELLANT 1

PROPELLANT TYPE	LOVA XM39 LOTA2-202
MASS OF PROPELLANT (LBM)	13.3500
DENSITY OF PROPELLANT (LBM/IN**3)	0.0584
FORM FUNCTION INDICATOR	9
OUTSIDE DIAMETER (INS)	0.3060
INSIDE DIAMETER (INS)	0.0150
LENGTH (INS)	0.3400
NUMBER OF PERFORATIONS	19.
SLOT WIDTH (NFORM=11) OR SCROLL DIA. (NFORM=13) (INS)	0.0000
PROPELLANT STACKED (0=NO,1=YES)	0
ATTACHMENT CONDITION (0=FREE,1=ATTACHED TO TUBE, 2=ATTACHED TO PROJECTILE)	0
BOND STRENGTH (LBF) (N.B. ZERO DEFAULTS TO INFINITY)	0.000000
DRAG RELAXATION EXPONENT (STACKED GRANULAR ONLY)	1.000
INITIAL DRAG MULTIPLIER (STACKED GRANULAR ONLY)	0.000
TIME DELAY FOR TUMBLING (STACKED GRANULAR ONLY) (MSEC)	0.000
GRAIN INHIBITED ON OUTER SURFACE (0=NO,1=YES)	0

RHEOLOGICAL PROPERTIES

SPEED OF COMPRESSION WAVE IN SETTLED BED (IN/SEC)	17400.
SETTLING POROSITY	0.5000
SPEED OF EXPANSION WAVE (IN/SEC)	50000.
POISSON RATIO (-)	0.5000

SOLID PHASE THERMOCHEMISTRY

MAXIMUM PRESSURE FOR BURN RATE DATA (LBF/IN**2)	6000.
BURNING RATE PRE-EXPONENTIAL FACTOR (IN/SEC/PSI**BN)	0.6457E-04
BURNING RATE EXPONENT	1.1090
MAXIMUM PRESSURE FOR BURN RATE DATA (LBF/IN**2)	20000.
BURNING RATE PRE-EXPONENTIAL FACTOR (IN/SEC/PSI**BN)	0.6682E-02
BURNING RATE EXPONENT	0.5757

MAXIMUM PRESSURE FOR BURN RATE DATA (LBF/IN**2)	100000.
BURNING RATE PRE-EXPONENTIAL FACTOR (IN/SEC/PSI**BN)	0.2030E-04
BURNING RATE EXPONENT	1.1610
BURNING RATE CONSTANT (IN/SEC)	0.0000
IGNITION TEMPERATURE (DEG.R)	858.0
THERMAL CONDUCTIVITY (LBF/SEC/DEG.R)	0.2770E-01
THERMAL DIFFUSIVITY (IN**2/SEC)	0.1345E-03
EMISSIVITY FACTOR	0.600

GAS PHASE THERMOCHEMISTRY

CHEMICAL ENERGY RELEASED IN BURNING(LBF-IN/LBM)	.15250E+08
MOLECULAR WEIGHT (LBM/LBMOL)	21.1690
RATIO OF SPECIFIC HEATS	1.2812
COVOLUME	28.4400

LOCATION OF PACKAGE(S)

PACKAGE	LEFT BDDY(INS)	RIGHT BDDY(INS)	MASS(LBM)	INNER RADIUS(IN)	OUTER RADIUS(IN)
1	0.000	21.622	13.350	0.000	0.000

PROPERTIES OF PRIMER

CHEMICAL ENERGY RELEASED IN BURNING(LBF-IN/LBM)	0.9997E+07
MOLECULAR WEIGHT (LBM/LBMOL)	29.8200
RATIO OF SPECIFIC HEATS	1.2254
SPECIFIC VOLUME OF SOLID(IN**3/LBM)	16.7800

PRIMER DISCHARGE FUNCTION (LBM/IN/SEC)

POS.(INS)	3.00	11.00
TIME(SEC)		
0.000	4.41	4.41
0.400E-02	0.00	0.00

PARAMETERS TO SPECIFY TUBE GEOMETRY

DISTANCE(IN)	RADIUS(IN)
0.000	2.000
3.000	2.500
18.500	2.410
21.500	2.097
24.900	2.097
210.500	2.097

BORE RESISTANCE TABLE

POSITION(INS)	RESISTANCE(PSI)

21.622	100.
22.622	2000.
24.500	500.
210.500	500.

THERMAL PROPERTIES OF TUBE

THERMAL CONDUCTIVITY (LBF/SEC/DEG.R)	0.0000
THERMAL DIFFUSIVITY (IN**2/SEC)	0.0000
EMISSIVITY FACTOR	0.000
INITIAL TEMPERATURE (DEG.R)	500.00

PROJECTILE AND RIFLING DATA

INITIAL POSITION OF BASE OF PROJECTILE(INS)	21.622
MASS OF PROJECTILE (LBM)	23.200
POLAR MOMENT OF INERTIA (LBM-IN**2)	44.000
ANGLE OF RIFLING (DEG)	9.900
PROPULSION AREA (IN**2)	0.000

POSITIONS FOR PRESSURE TABLE STORAGE

0.0000 21.6220

CHEMISTRY OPTION DATA

NUMBER OF SPECIES	5
NUMBER OF GAS-PHASE REACTIONS	2
NUMBER OF SOLID-PHASE REACTIONS	0

PROPERTIES OF SPECIES

NAME	PHASE	CV LBF-IN/LBM-R	CP LBF-IN/LBM-R	COVOLUME IN**3/LBM	MOL.WGT LB/LBMOL	DENSITY LBM/IN**3	TRANSFER COEF.	KTEQL
LOVA-I	G	3498.0	4481.0	28.640	20.954	0.00000	0.00000	0
BENITE	G	2867.5	3513.8	23.230	29.820	0.00000	0.00000	0
BENITE	S	2867.5	2867.5	0.000	0.000	0.06000	0.00000	0
AIR	G	1604.9	2246.9	26.680	28.896	0.00000	0.00000	0
LOVA-F	G	3498.0	4481.0	28.640	20.954	0.00000	0.00000	0

COMPOSITION OF LOCAL COMBUSTION PRODUCTS OF PROPELLANT 1

ENERGY	MASS FRACTIONS (-)									
LBF-IN/LBM	YO(1)	YO(2)	YO(3)	YO(4)	YO(5)	YO(6)	YO(7)	YO(8)	YO(9)	YO(10)
7625000.	1.00000	0.00000	0.00000	0.00000	0.00000					

COMPOSITION OF COMBUSTION PRODUCTS OF IGNITER

ENERGY	MASS FRACTIONS (-)									
LBF-IN/LBM	YO(1)	YO(2)	YO(3)	YO(4)	YO(5)	YO(6)	YO(7)	YO(8)	YO(9)	YO(10)
9997373.	0.00000	1.00000	0.00000	0.00000	0.00000					

COMPOSITION OF AMBIENT GAS

ENERGY	MASS FRACTIONS (-)									
LBF-IN/LBM	YO(1)	YO(2)	YO(3)	YO(4)	YO(5)	YO(6)	YO(7)	YO(8)	YO(9)	YO(10)
882690.	0.00000	0.00000	0.00000	1.00000	0.00000					

GAS-PHASE REACTION DATA

REACTION 1

REACTANT SPECIES	1	0	0	0	PRODUCT SPECIES	5	0	0	0
STOICHIOMETRIC COEFFICIENTS (LBM)	1.000	0.000	0.000	0.000		1.000	0.000	0.000	0.000
HEAT OF REACTION (LBF-IN/LBM)			7625000.						
RATE COEFFICIENT (UNITS YIELD LBM/IN**3/SEC)			0.145E+08						
RATE TEMPERATURE EXPONENT (-)			0.000						
RATE ACTIVATION ENERGY (LBF-IN/LBMOL)			300000000.000						
REACTION ORDER WITH RESPECT TO REACTANTS (-)	1.000	0.000	0.000	0.000	1.000				

REACTION 2

REACTANT SPECIES	1	2	0	0	PRODUCT SPECIES	5	2	0	0
STOICHIOMETRIC COEFFICIENTS (LBM)	1.000	1.000	0.000	0.000		1.000	1.000	0.000	0.000
HEAT OF REACTION (LBF-IN/LBM)			7625000.						
RATE COEFFICIENT (UNITS YIELD LBM/IN**3/SEC)			0.145E+10						
RATE TEMPERATURE EXPONENT (-)			0.000						
RATE ACTIVATION ENERGY (LBF-IN/LBMOL)			300000000.000						
REACTION ORDER WITH RESPECT TO REACTANTS (-)	1.000	1.000	0.000	0.000	0.000				

NOVSUB MESSAGE... SETTLING POROSITY AT REFERENCE COMPOSITION HAS BEEN
DEFAULTED TO 0.41413 TO AVOID INITIAL BED COMPACTION OF PROPELLANT TYPE 1

EQUIVALENT INTBAL DATA

PROJECTILE TRAVEL(IN)	188.000
CHAMBER VOLUME(IN**3)	391.050
GUN MASS(LBM)	0.100E+21
GUN RES. FAC.	0.000
ELEV. ANGLE(DEG)	0.000
PROJECTILE MASS(LBM)	23.505

PROJECTILE TRAV. (IN)	RESISTANCE(PSI)
0.000	100.000

1.000	2000.000
2.878	500.000
188.878	500.000

VEL. THRESHOLD FOR DYN. RES.(F/S)	27.000
VEL. DEPENDENCE ON CHARGE WEIGHT(F/S/LBM)	0.000
ESTIMATED MUZZLE VELOCITY(F/S)	0.000
N.B. USE VALUE FROM SUMMARY TABLE. INTBAL WILL NOT ACCEPT ZERO	
BORE AREA(IN**2)	13.815
AIR DENSITY(LBM/FT**3)	0.000
IGNITER MASS(LBM)	0.0715
FLAME TEMPERATURE(K)	2012.402
RATIO OF SPECIFIC HEATS(-)	1.2254
IMPETUS(LBF-IN/LBM)	2253323.8
INITIAL CHARGE WEIGHT(LBM)	13.350
FINAL CHARGE WEIGHT(LBM)	13.350
CHARGE WEIGHT INCREMENT(LBM)	1.000
FLAME TEMPERATURE(K)	2718.749
RATIO OF SPECIFIC HEATS(-)	1.2812
IMPETUS(LBF-IN/LBM)	4288300.0
INITIAL TEMPERATURE(K)	277.8
DENSITY(LBM/IN**3)	0.05845
COVOLUME(IN**3/LBM)	28.440

COEFF(IN/S/PSI**N)	EXPONENT(-)	UPPER PRES. LIM. (PSI)
0.6457E-04	1.109	6000.
0.6682E-02	0.5757	0.2000E+05
0.2030E-04	1.161	0.1000E+06

LENGTH OF GRAIN(IN)	0.3400
EXTERNAL DIAMETER(IN)	0.3060
CENTER PERF. DIAMETER(IN)	0.0150
OUTER PERF. DIAMETER(IN)	0.0150
DIST. BETWEEN PERF. CENTERS(IN)	0.0802
OFFSET(IN)	0.0000
ANGLE(DEG)	0.0000
INTEGRATION STEP(MSEC)	0.2500
PRINT STEP(MSEC)	1.0000

INTENTIONALLY LEFT BLANK.

Appendix B

XNOVAKTC Input Data for 120-mm, M829 Cartridge

INTENTIONALLY LEFT BLANK.

XNOVAKTC: INPUT FILE CARD IMAGE

```
M829, comb. case, ambient, bayonet primer, granular, x829ab
TFFFTTT        1 1 0      10
   99 3500    0 3500          .001
.0045      186.9      0.0001     2.0        0.05       0.01       0.0001     0.0001
    6    9    6    7    0    0    1    2    0    0    0    8
    0
529.        14.7       28.896     1.4
529.0                                                                    10.0
JA2 7PF LOT 472-138  0.0        22.2       17.90      .05709
    7    .415     0.040       .643       7.
10000.      1.0        50000.                .5
10000.      .00400     .7162      100000.    .0008881   .8796      0.0        800.
.0277       .0001345   .6
20372433.  24.8226     1.2268     26.98
9967547.    30.93      1.221      23.00
0.          .00025     .00125     .0015      .0035      .00375     .005       .00525
.00725
0.0         1.0        3.0        3.01       12.0       12.1
0.0         0.0        0.0        0.0        0.0        0.0
0.0         0.0        0.0        6.24       0.0        0.0
0.0         0.0        0.0        6.24       6.24       0.0
 0.          0.        0.0        0.0        6.24       0.
 0.          0.        0.0        0.0        0.         0.
 0.          0.        0.         0.         0.         0.
 0.          0.        0.         0.         0.         0.
0.0         0.0        0.0        0.0        0.0        0.0
0.0         0.0        0.0        0.0        0.0        0.0
0.0         2.25         3.0      3.09       19.0       3.09       22.00      2.38
23.37       2.36       208.35     2.36
0.00        145.       0.24       835.       0.35       930.0      0.47       835.
0.95        510.       3.94       290.       187.       0.0
7.77        0.0228     .7
22.2        15.65      44.0       0.000
0.0         22.2       30.        41.        60.        90.        120.        19.

    2    2    0    0    0    0    0    2
0.0          0.53       8.0        1.28
    3    4    4
0.0         0.145      18.0       0.145      22.2       0.005
    1    2
0.0295      14.7       0.0455     11000.     .0497      25000.     .0548      100000.
    2    0
10000.      0.000160      1.301      100000.    13.55      .0690
0.0         800.       .0277      .0001345
9300000.    22.39      1.258
0.0295      14.7       0.0455     11000.     .0497      25000.     .0548      100000.
    1    0
100000.     0.00006252    1.301
0.0         80000.     .0277      .0001345
9300000.    22.39      1.258
```

M829, comb. case, ambient, bayonet primer, granular, x829ab

XNOVAKTC VERSION NUMBER 188.001

CONTROL DATA

LOGICAL VARIABLES:
PRINT T DISK WRITE F DISK READ F
I.B. TABLE T FLAME TABLE T PRESSURE TABLE(S) T
EROSIVE EFFECT 0 WALL TEMPERATURE CALCULATION 0
BED PRECOMPRESSED 0
HEAT LOSS CALCULATION 1

BORE RESISTANCE FUNCTION 1
TRAVELING CHARGE OPTION (0=NO,1=YES) 0
CONSERVATIVE SCHEME TO INTEGRATE SOLID-PHASE CONTINUITY EQUATION (0=NO,OLD; 1=YES,NEW) 0
KINETICS MODE (0=NONE;1=GAS-PHASE ONLY;2=BOTH PHASES) 0
TANK GUN OPTION (0=NO,1=YES) 1
INPUT ECHO OPTION 0
FORWARD BOUNDARY CONDITION (0=CLOSED;1=OPEN;2=ROCKET) 0

INTEGRATION PARAMETERS

NUMBER OF STATIONS AT WHICH DATA ARE STORED	99
NUMBER OF STEPS BEFORE LOGOUT	3500
TIME STEP FOR DISK START	0
NUMBER OF STEPS FOR TERMINATION	3500
TIME INTERVAL BEFORE LOGOUT(SEC)	0.1000E-02
TIME FOR TERMINATION (SEC)	0.4500E-02
PROJECTILE TRAVEL FOR TERMINATION (INS)	186.90
MAXIMUM TIME STEP (SEC)	0.1000E-03
STABILITY SAFETY FACTOR	2.00
SOURCE STABILITY FACTOR	0.0500
SPATIAL RESOLUTION FACTOR	0.0100
TIME INTERVAL FOR I.B. TABLE STORAGE(SEC)	0.1000E-03
TIME INTERVAL FOR PRESSURE TABLE STORAGE (SEC)	0.1000E-03

FILE COUNTERS

NUMBER OF STATIONS TO SPECIFY TUBE RADIUS	6
NUMBER OF TIMES TO SPECIFY PRIMER DISCHARGE	9
NUMBER OF POSITIONS TO SPECIFY PRIMER DISCHARGE	6
NUMBER OF ENTRIES IN BORE RESISTANCE TABLE	7
NUMBER OF ENTRIES IN WALL TEMPERATURE TABLE	0
NUMBER OF ENTRIES IN FORWARD FILLER ELEMENT TABLE	0
NUMBER OF TYPES OF PROPELLANTS	1
NUMBER OF BURN RATE DATA SETS	2
NUMBER OF ENTRIES IN VOID FRACTION TABLE(S)	0 0 0
NUMBER OF ENTRIES IN PRESSURE HISTORY TABLES	8
NUMBER OF ENTRIES IN REAR FILLER ELEMENT TABLE	0

GENERAL PROPERTIES OF INITIAL AMBIENT GAS

INITIAL TEMPERATURE (DEG.R)	529.0
INITIAL PRESSURE (PSI)	14.7
MOLECULAR WEIGHT (LBM/LBMOL)	28.896
RATIO OF SPECIFIC HEATS	1.4000

GENERAL PROPERTIES OF PROPELLANT BED

INITIAL TEMPERATURE (DEG.R)	529.0

PROPERTIES OF PROPELLANT 1

PROPELLANT TYPE	JA2 7PF LOT 472-138
MASS OF PROPELLANT (LBM)	17.9000
DENSITY OF PROPELLANT (LBM/IN**3)	0.0571
FORM FUNCTION INDICATOR	7
OUTSIDE DIAMETER (INS)	0.4150
INSIDE DIAMETER (INS)	0.0400
LENGTH (INS)	0.6430
NUMBER OF PERFORATIONS	7.
SLOT WIDTH (NFORM=11) OR SCROLL DIA. (NFORM=13) (INS)	0.0000
PROPELLANT STACKED (0=NO,1=YES)	0
ATTACHMENT CONDITION (0=FREE,1=ATTACHED TO TUBE, 2=ATTACHED TO PROJECTILE)	0
BOND STRENGTH (LBF) (N.B. ZERO DEFAULTS TO INFINITY)	0.000000
GRAIN INHIBITED ON OUTER SURFACE (0=NO,1=YES)	0

RHEOLOGICAL PROPERTIES

SPEED OF COMPRESSION WAVE IN SETTLED BED (IN/SEC)	10000.
SETTLING POROSITY	1.0000
SPEED OF EXPANSION WAVE (IN/SEC)	50000.
POISSON RATIO (-)	0.5000

SOLID PHASE THERMOCHEMISTRY

MAXIMUM PRESSURE FOR BURN RATE DATA (LBF/IN**2)	10000.
BURNING RATE PRE-EXPONENTIAL FACTOR (IN/SEC/PSI**BN)	0.4000E-02
BURNING RATE EXPONENT	0.7162
MAXIMUM PRESSURE FOR BURN RATE DATA (LBF/IN**2)	100000.
BURNING RATE PRE-EXPONENTIAL FACTOR (IN/SEC/PSI**BN)	0.8881E-03
BURNING RATE EXPONENT	0.8796
BURNING RATE CONSTANT (IN/SEC)	0.0000
IGNITION TEMPERATURE (DEG.R)	800.0
THERMAL CONDUCTIVITY (LBF/SEC/DEG.R)	0.2770E-01
THERMAL DIFFUSIVITY (IN**2/SEC)	0.1345E-03
EMISSIVITY FACTOR	0.600

GAS PHASE THERMOCHEMISTRY

CHEMICAL ENERGY RELEASED IN BURNING(LBF-IN/LBM)	.20372E+08
MOLECULAR WEIGHT (LBM/LBMOL)	24.8226
RATIO OF SPECIFIC HEATS	1.2268
COVOLUME	26.9800

LOCATION OF PACKAGE(S)

PACKAGE	LEFT BDDY(INS)	RIGHT BDDY(INS)	MASS(LBM)	INNER RADIUS(IN)	OUTER RADIUS(IN)
1	0.000	22.200	17.900	0.000	0.000

PROPERTIES OF PRIMER

CHEMICAL ENERGY RELEASED IN BURNING(LBF-IN/LBM)	0.9968E+07
MOLECULAR WEIGHT (LBM/LBMOL)	30.9300
RATIO OF SPECIFIC HEATS	1.2210
SPECIFIC VOLUME OF SOLID(IN**3/LBM)	23.0000

PRIMER DISCHARGE FUNCTION (LBM/IN/SEC)

POS.(INS)	0.00	1.00	3.00	3.01	12.00	12.10
TIME(SEC)						
0.000	0.00	0.00	0.00	0.00	0.00	0.00
0.250E-03	0.00	0.00	0.00	6.24	0.00	0.00
0.125E-02	0.00	0.00	0.00	6.24	6.24	0.00
0.150E-02	0.00	0.00	0.00	0.00	6.24	0.00
0.350E-02	0.00	0.00	0.00	0.00	0.00	0.00
0.375E-02	0.00	0.00	0.00	0.00	0.00	0.00
0.500E-02	0.00	0.00	0.00	0.00	0.00	0.00
0.525E-02	0.00	0.00	0.00	0.00	0.00	0.00
0.725E-02	0.00	0.00	0.00	0.00	0.00	0.00

PARAMETERS TO SPECIFY TUBE GEOMETRY

DISTANCE(IN)	RADIUS(IN)
0.000	2.250
3.000	3.090
19.000	3.090
22.000	2.380
23.370	2.360
208.350	2.360

BORE RESISTANCE TABLE

POSITION(INS)	RESISTANCE(PSI)
0.000	145.
0.240	835.
0.350	930.
0.470	835.
0.950	510.
3.940	290.
187.000	0.

THERMAL PROPERTIES OF TUBE

THERMAL CONDUCTIVITY (LBF/SEC/DEG.R)	7.770
THERMAL DIFFUSIVITY (IN**2/SEC)	0.2280E-01
EMISSIVITY FACTOR	0.700
INITIAL TEMPERATURE (DEG.R)	529.00

PROJECTILE AND RIFLING DATA

INITIAL POSITION OF BASE OF PROJECTILE(INS)	22.200
MASS OF PROJECTILE (LBM)	15.650
POLAR MOMENT OF INERTIA (LBM-IN**2)	44.000
ANGLE OF RIFLING (DEG)	0.000

POSITIONS FOR PRESSURE TABLE STORAGE

0.0000	22.2000	30.0000	41.0000	60.0000	90.0000	120.0000	19.0000

LOCATION RELATIVE TO TUBE (0) OR REAR OF AFTERBODY (1)

0	0	0	0	0	0	0	0

TANK GUN OPTION DATA

NUMBER OF DATA TO DESCRIBE AFTERBODY	2
TUBE SURFACE SOURCE (0=NONE,1=TABULAR,2=MODELED)	2
CENTERLINE SOURCE (0=NONE,1=TABULAR,2=MODELED)	0
AFTERBODY SURFACE SOURCE (0=NONE,1=TABULAR,2=MODELED)	0
NUMBER OF ENDWALL DATA SETS	0
NUMBER OF PERMEABILITY DATA SETS	0
NUMBER OF REACTIVITY DATA SETS	0
NUMBER OF SEGMENTS ON TUBE SURFACE SOURCE	2
NUMBER OF SEGMENTS ON CENTERLINE SURFACE SOURCE	0
NUMBER OF SEGMENTS ON AFTERBODY SURFACE SOURCE	0
CONTROL CHARGE PRESENT (0=NO;1=YES)	0
NUMBER OF DATA TO DEFINE EXTERNAL GEOMETRY OF CONTROL CHARGE CHAMBER	0
CONTROL CHARGE DETERRED (0=NO;1=YES)	0

GEOMETRY OF AFTERBODY

AXIAL POS.(IN)	RADIUS(IN)
0.000	0.530
8.000	1.280

DESCRIPTION OF TUBE SURFACE SOURCE

NUMBER OF DATA TO DESCRIBE THICKNESS OF LAYER	3
NUMBER OF DATA TO DESCRIBE DENSITY OF SEGMENT 1	4
NUMBER OF DATA TO DESCRIBE DENSITY OF SEGMENT 2	4
NUMBER OF DATA TO DESCRIBE DENSITY OF SEGMENT 3	0

THICKNESS OF REACTIVE LAYER

AXIAL POS.(IN)	THICKNESS(IN)	SEGMENT
0.000	0.145	1
18.000	0.145	2

22.200 0.005 0

PROPERTIES OF SEGMENT NUMBER 1

DENSITY OF REACTIVE LAYER

DENSITY(LBM/IN**3)	PRESSURE(PSI)
0.0295	15.
0.0455	11000.
0.0497	25000.
0.0548	100000.

NUMBER OF DATA TO DESCRIBE BURN RATE 2

BURN RATE DATA

MAX.PRESS(PSI)	COEFF(IN/SEC/PSI**BN)	EXPONENT
10000.	0.16000E-03	1.3010
100000.	13.550	0.0690

BURN RATE ADDITIVE CONSTANT (IN/SEC)	0.0000
IGNITION TEMPERATURE (R)	800.0
THERMAL CONDUCTIVITY (LBF/SEC/R)	0.2770E-01
THERMAL DIFFUSIVITY (IN**2/SEC)	0.1345E-03

CHEMICAL ENERGY (LBF-IN/LBM)	.93000E+07
MOLECULAR WEIGHT (LBM/LBMOL)	22.3900
RATIO OF SPECIFIC HEATS (-)	1.2580

PROPERTIES OF SEGMENT NUMBER 2

DENSITY OF REACTIVE LAYER

DENSITY(LBM/IN**3)	PRESSURE(PSI)
0.0295	15.
0.0455	11000.
0.0497	25000.
0.0548	100000.

NUMBER OF DATA TO DESCRIBE BURN RATE 1

BURN RATE DATA

MAX.PRESS(PSI)	COEFF(IN/SEC/PSI**BN)	EXPONENT

100000.	0.62520E-04	1.3010

BURN RATE ADDITIVE CONSTANT (IN/SEC)	0.0000
IGNITION TEMPERATURE (R)	80000.0
THERMAL CONDUCTIVITY (LBF/SEC/R)	0.2770E-01
THERMAL DIFFUSIVITY (IN**2/SEC)	0.1345E-03

CHEMICAL ENERGY (LBF-IN/LBM)	.93000E+07
MOLECULAR WEIGHT (LBM/LBMOL)	22.3900
RATIO OF SPECIFIC HEATS (-)	1.2580

BORE RESISTANCE DATA HAVE BEEN INTERPRETED AS RELATIVE TO PROJECTILE DISPLACEMENT.
NOVSUB MESSAGE... SETTLING POROSITY AT REFERENCE COMPOSITION HAS BEEN DEFAULTED TO 0.42399 TO AVOID INITIAL BED COMPACTI
OF PROPELLANT TYPE 1
VOLUME OF AFTERBODY (IN**3) 21.762

EQUIVALENT INTBAL DATA

PROJECTILE TRAVEL(IN)	186.900
CHAMBER VOLUME(IN**3)	622.132
GUN MASS(LBM)	0.100E+21
GUN RES. FAC.	0.000
ELEV. ANGLE(DEG)	0.000
PROJECTILE MASS(LBM)	15.650

PROJECTILE TRAV. (IN)	RESISTANCE(PSI)
0.000	145.000
0.240	835.000
0.350	930.000
0.470	835.000
0.950	510.000
3.940	290.000
187.000	0.000

VEL. THRESHOLD FOR DYN. RES.(F/S)	27.000
VEL. DEPENDENCE ON CHARGE WEIGHT(F/S/LBM)	0.000
ESTIMATED MUZZLE VELOCITY(F/S)	0.000
N.B. USE VALUE FROM SUMMARY TABLE. INTBAL WILL NOT ACCEPT ZERO	
BORE AREA(IN**2)	17.497
AIR DENSITY(LBM/FT**3)	0.000
IGNITER MASS(LBM)	0.0849
FLAME TEMPERATURE(K)	2040.535
RATIO OF SPECIFIC HEATS(-)	1.2210
IMPETUS(LBF-IN/LBM)	2202827.9

INITIAL CHARGE WEIGHT(LBM)	17.900
FINAL CHARGE WEIGHT(LBM)	17.900
CHARGE WEIGHT INCREMENT(LBM)	1.000
FLAME TEMPERATURE(K)	3434.921
RATIO OF SPECIFIC HEATS(-)	1.2268
IMPETUS(LBF-IN/LBM)	4620467.8
INITIAL TEMPERATURE(K)	293.9
DENSITY(LBM/IN**3)	0.05709
COVOLUME(IN**3/LBM)	26.980

EQUIVALENT INTBAL DATA (CONTINUED)

COEFF(IN/S/PSI**N)	EXPONENT(-)	UPPER PRES. LIM. (PSI)
0.4000E-02	0.7162	0.1000E+05
0.8881E-03	0.8796	0.1000E+06

LENGTH OF GRAIN(IN)	0.6430
EXTERNAL DIAMETER(IN)	0.4150
CENTER PERF. DIAMETER(IN)	0.0400
OUTER PERF. DIAMETER(IN)	0.0400
DIST. BETWEEN PERF. CENTERS(IN)	0.1137
OFFSET(IN)	0.0000
ANGLE(DEG)	0.0000

INTEGRATION STEP(MSEC)	0.2500
PRINT STEP(MSEC)	1.0000

No of Copies	Organization
1	Office of the Secretary of Defense OUSD(A) Director, Live Fire Testing ATTN: James F. O'Bryon Washington, DC 20301-3110
2	Administrator Defense Technical Info Center ATTN: DTIC-DDA Cameron Station Alexandria, VA 22304-6145
1	HQDA (SARD-TR) WASH DC 20310-0001
1	Commander US Army Materiel Command ATTN: AMCDRA-ST 5001 Eisenhower Avenue Alexandria, VA 22333-0001
1	Commander US Army Laboratory Command ATTN: AMSLC-DL Adelphi, MD 20783-1145
2	Commander US Army, ARDEC ATTN: SMCAR-IMI-I Picatinny Arsenal, NJ 07806-5000
2	Commander US Army, ARDEC ATTN: SMCAR-TDC Picatinny Arsenal, NJ 07806-5000
1	Director Benet Weapons Laboratory US Army, ARDEC ATTN: SMCAR-CCB-TL Watervliet, NY 12189-4050
1	Commander US Army Armament, Munitions and Chemical Command ATTN: SMCAR-ESP-L Rock Island, IL 61299-5000
1	Commander US Army Aviation Systems Command ATTN: AMSAV-DACL 4300 Goodfellow Blvd. St. Louis, MO 63120-1798

No of Copies	Organization
1	Director US Army Aviation Research and Technology Activity Ames Research Center Moffett Field, CA 94035-1099
1	Commander US Army Missile Command ATTN: AMSMI-RD-CS-R (DOC) Redstone Arsenal, AL 35898-5010
1	Commander US Army Tank-Automotive Command ATTN: AMSTA-TSL (Technical Library) Warren, MI 48397-5000
1	Director US Army TRADOC Analysis Command ATTN: ATAA-SL White Sands Missile Range, NM 88002-5502
(Class. only) 1	Commandant US Army Infantry School ATTN: ATSH-CD (Security Mgr.) Fort Benning, GA 31905-5660
(Unclass. only) 1	Commandant US Army Infantry School ATTN: ATSH-CD-CSO-OR Fort Benning, GA 31905-5660
1	Air Force Armament Laboratory ATTN: AFATL/DLODL Eglin AFB, FL 32542-5000
	Aberdeen Proving Ground
2	Dir, USAMSAA ATTN: AMXSY-D AMXSY-MP, H. Cohen
1	Cdr, USATECOM ATTN: AMSTE-TD
3	Cdr, CRDEC, AMCCOM ATTN: SMCCR-RSP-A SMCCR-MU SMCCR-MSI
1	Dir, VLAMO ATTN: AMSLC-VL-D

No. of Copies	Organization
1	Commander USA Concepts Analysis Agency ATTN: D. Hardison 8120 Woodmont Avenue Bethesda, MD 20014-2797
1	C.I.A. 01R/DB/Standard Washington, DC 20505
1	US Army Ballistic Missile Defense Systems Command Advanced Technology Center P.O. Box 1500 Huntsville, AL 35807-3801
1	Chairman DoD Explosives Safety Board Room 856-C Hoffman Bldg. 1 2461 Eisenhower Avenue Alexandria, VA 22331-0600
1	Commander US Army Materiel Command ATTN: AMCPM-GCM-WF 5001 Eisenhower Avenue Alexandria, VA 22333-5001
1	Commander US Army Materiel Command ATTN: AMCDE-DW 5001 Eisenhower Avenue Alexandria, VA 22333-5001
4	Project Manager Autonomous Precision-Guided Munition (APGM) Armament RD&E Center US Army AMCCOM ATTN: AMCPM-CW AMCPM-CWW AMCPM-CWS, M. Fisette AMCPM-CWA-S, R. DeKleine Picatinny Arsenal, NJ 07806-5000
2	Project Manager Production Base Modernization Agency ATTN: AMSMC-PBM, A. Siklosi AMSMC-PBM-E, L. Laibson Picatinny Arsenal, NJ 07806-5000

No. of Copies	Organization
3	PEO-Armaments Project Manger Tank Main Armament Systems ATTN: AMCPM-TMA, K. Russell AMCPM-TMA-105 AMCPM-TMA-120 Picatinny Arsenal, NJ 07806-5000
1	Commander Armament RD&E Center US Army AMCCOM ATTN: SMCAR-AEE Picatinny Arsenal, NJ 07806-5000
8	Commander Armament RD&E Center US Army AMCCOM ATTN: SMCAR-AEE-B A. Beardell B. Brodman D. Downs S. Einstein S. Westley S. Bernstein C. Roller J. Rutkowski Picatinny Arsenal, NJ 07806-5000
2	Commander US Army ARDEC ATTN: SMCAR-AES, S. Kaplowitz; D. Spring Picatinny Arsenal, NJ 07806-5000
2	Commander Armament RD&E Center US Army AMCCOM ATTN: SMCAR-HFM, E. Barrieres SMCAR-CCH-V, C. Mandala Picatinny Arsenal, NJ 07806-5000
1	Commander Armament RD&E Center US Army AMCCOM ATTN: SMCAR-FSA-T, M. Salsbury Picatinny Arsenal, NJ 07806-5000
1	Commander, USACECOM R&D Technical Library ATTN: ASQNC-ELC-I-T, Myer Center Fort Monmouth, NJ 07703-5301

No. of Copies	Organization
1	Commander US Army Harry Diamond Laboratories ATTN: SLCHD-TA-L 2800 Powder Mill Rd Adelphi, MD 20783-1145
1	Commandant US Army Aviation School ATTN: Aviation Agency Fort Rucker, AL 36360
1	Project Manager US Army Tank-Automotive Command Improved TOW Vehicle ATTN: AMCPM-ITV Warren, MI 48397-5000
2	Program Manager US Army Tank-Automotive Command ATTN: AMCPM-ABMS, T. Dean Warren, MI 48092-2498
1	Project Manager US Army Tank-Automotive Command Fighting Vehicle Systems ATTN: AMCPM-BFVS Warren, MI 48092-2498
1	President US Army Armor and Engineer Board ATTN: ATZK-AD-S Fort Knox, KY 40121-5200
1	Project Manager US Army Tank-Automotive Command M-60 Tank Development ATTN: AMCPM-ABMS Warren, MI 48092-2498
1	Commander US Army Training and Doctrine Command ATTN: ATCD-MA, MAJ Williams Fort Monroe, VA 23651
2	Director US Army Materials Technology Laboratory ATTN: SLCMT-ATL Watertown, MA 02172-0001
1	Commander US Army Research Office ATTN: Technical Library P. O. Box 12211 Research Triangle Park, NC 27709-2211

No. of Copies	Organization
1	Commander US Army Belvoir Research and Development Center ATTN: STRBE-WC Fort Belvoir, VA 22060-5006
1	Director US Army TRAC-Ft Lee ATTN: ATRC-L, (Mr. Cameron) Fort Lee, VA 23801-6140
1	Commandant US Army Command and General Staff College Fort Leavenworth, KS 66027
1	Commandant US Army Special Warfare School ATTN: Rev and Tng Lit Div Fort Bragg, NC 28307
3	Commander Radford Army Ammunition Plant ATTN: SMCAR-QA/HI LIB Radford, VA 24141-0298
1	Commander US Army Foreign Science and Technology Center ATTN: AMXST-MC-3 220 Seventh Street, NE Charlottesville, VA 22901-5396
2	Commander Naval Sea Systems Command ATTN: SEA 62R SEA 64 Washington, DC 20362-5101
1	Commander Naval Air Systems Command ATTN: AIR-954-Technical Library Washington, DC 20360
1	Assistant Secretary of the Navy (R, E, and S) ATTN: R. Reichenbach Room 5E787 Pentagon Bldg Washington, DC 20375

No. of Copies	Organization
1	Naval Research Laboratory Technical Library Washington, DC 20375
1	Commandant US Army Command and General Staff College Fort Leavenworth, KS 66027
2	Commandant US Army Field Artillery Center and School ATTN: ATSF-CO-MW, B. Willis Ft. Sill, OK 73503-5600
1	Office of Naval Research ATTN: Code 473, R. S. Miller 800 N. Quincy Street Arlington, VA 22217-9999
3	Commandant US Army Armor School ATTN: ATZK-CD-MS, M. Falkovitch Armor Agency Fort Knox, KY 40121-5215
2	Commander US Naval Surface Warfare Center ATTN: J. P. Consaga C. Gotzmer Indian Head, MD 20640-5000
4	Commander Naval Surface Warfare Center ATTN: Code 240, S. Jacobs Code 730 Code R-13, K. Kim R. Bernecker Silver Spring, MD 20903-5000
2	Commanding Officer Naval Underwater Systems Center ATTN: Code 5B331, R. S. Lazar Technical Library Newport, RI 02840
5	Commander Naval Surface Warfare Center ATTN: Code G33, J. L. East W. Burrell J. Johndrow Code G23, D. McClure Code DX-21 Technical Library Dahlgren, VA 22448-5000

No. of Copies	Organization
3	Commander Naval Weapons Center ATTN: Code 388, C. F. Price Code 3895, T. Parr Information Science Division China Lake, CA 93555-6001
1	Program Manager AFOSR Directorate of Aerospace Sciences ATTN: L. H. Caveny Bolling AFB Washington, DC 20332-0001
5	Commander Naval Ordnance Station ATTN: L. Torreyson T. C. Smith D. Brooks W. Vienna Technical Library Indian Head, MD 20640-5000
1	AL/TSTL (Technical Library) ATTN: J. Lamb Edwards AFB, CA 93523-5000
1	AFSC/SDOA Andrews AFB, MD 20334
1	AFATL/DLYV Eglin AFB, FL 32542-5000
1	AFATL/DLXP Eglin AFB, FL 32542-5000
1	AFATL/DLJE Eglin AFB, FL 32542-5000
1	NASA/Lyndon B. Johnson Space Center ATTN: NHS-22 Library Section Houston, TX 77054
1	AFELM, The Rand Corporation ATTN: Library D 1700 Main Street Santa Monica, CA 90401-3297
3	AAI Corporation ATTN: J. Herbert J. Frankle D. Cleveland P. O. Box 126 Hunt Valley, MD 21030-0126

No. of Copies	Organization
1	Aerojet Ordnance Company ATTN: D. Thatcher 2521 Michelle Drive Tustin, CA 92680-7014
1	Aerojet Solid Propulsion Company ATTN: P. Micheli Sacramento, CA 96813
1	Atlantic Research Corporation ATTN: M. King 5390 Cherokee Avenue Alexandria, VA 22312-2302
4	AL/LSCF ATTN: J. Levine L. Quinn D. Williams T. Edwards Edwards AFB, CA 93523-5000
1	AVCO Everett Research Laboratory ATTN: D. Stickler 2385 Revere Beach Parkway Everett, MA 02149-5936
2	Calspan Corporation ATTN: C. Murphy P. O. Box 400 Buffalo, NY 14225-0400
1	General Electric Company Armament Systems Department ATTN: M. J. Bulman 128 Lakeside Avenue Burlington, VT 05401-4985
1	IITRI ATTN: M. J. Klein 10 W. 35th Street Chicago, IL 60616-3799
1	Hercules, Inc. Allegheny Ballistics Laboratory ATTN: William B. Walkup P. O. Box 210 Rocket Center, WV 26726
1	Hercules, Inc. Radford Army Ammunition Plant ATTN: J. Pierce Radford, VA 24141-0299
3	Lawrence Livermore National Laboratory ATTN: L-355, A. Buckingham M. Finger L-324, M. Constantino P. O. Box 808 Livermore, CA 94550-0622
1	Olin Corporation Badger Army Ammunition Plant ATTN: R. J. Thiede Baraboo, WI 53913
1	Olin Corporation Smokeless Powder Operation ATTN: D. C. Mann P. O. Box 222 St. Marks, FL 32355-0222
1	Paul Gough Associates, Inc. ATTN: Dr. Paul S. Gough 1048 South Street Portsmouth, NH 03801
1	Physics International Company ATTN: Library, H. Wayne Wampler 2700 Merced Street San Leandro, CA 98457-5602
1	Princeton Combustion Research Laboratory, Inc. ATTN: M. Summerfield 475 US Highway One Monmouth Junction, NJ 08852-9650
2	Rockwell International Rocketdyne Division ATTN: BA08, J. E. Flanagan J. Gray 6633 Canoga Avenue Canoga Park, CA 91303-2703
3	Thiokol Corporation Huntsville Division ATTN: D. Flanigan Dr. John Deur Technical Library Huntsville, AL 35807

No. of Copies	Organization
2	Thiokol Corporation Elkton Division ATTN: R. Biddle Technical Library P. O. Box 241 Elkton, MD 21921-0241
1	Veritay Technology, Inc. ATTN: E. Fisher 4845 Millersport Highway East Amherst, NY 14501-0305
1	Universal Propulsion Company ATTN: H. J. McSpadden Black Canyon Stage 1 Box 1140 Phoenix, AZ 84029
1	Battelle Memorial Institute ATTN: Technical Library 505 King Avenue Columbus, OH 43201-2693
1	Brigham Young University Department of Chemical Engineering ATTN: M. Beckstead Provo, UT 84601
1	California Institute of Technology 204 Karman Laboratory Main Stop 301-46 ATTN: F.E.C. Culick 1201 E. California Street Pasadena, CA 91109
1	California Institute of Technology Jet Propulsion Laboratory ATTN: L. D. Strand, MS 512/102 4800 Oak Grove Drive Pasadena, CA 91109-8099
1	University of Illinois Department of Mechanical/Industrial Engineering ATTN: H. Krier 144 MEB; 1206 N. Green Street Urbana, IL 61801-2978
1	University of Massachusetts Department of Mechanical Engineering ATTN: K. Jakus Amherst, MA 01002-0014
1	University of Minnesota Department of Mechanical Engineering ATTN: E. Fletcher Minneapolis, MN 55414-3368
1	Case Western Reserve University Division of Aerospace Sciences ATTN: J. Tien Cleveland, OH 44135
3	Georgia Institute of Technology School of Aerospace Engineering ATTN: B.T. Zim E. Price W.C. Strahle Atlanta, GA 30332
1	Institute of Gas Technology ATTN: D. Gidaspow 3424 S. State Street Chicago, IL 60616-3896
1	Johns Hopkins University Applied Physics Laboratory Chemical Propulsion Information Agency ATTN: T. Christian Johns Hopkins Road Laurel, MD 20707-0690
1	Massachusetts Institute of Technology Department of Mechanical Engineering ATTN: T. Toong 77 Massachusetts Avenue Cambridge, MA 02139-4307
1	Pennsylvania State University Applied Research Laboratory ATTN: G.M. Faeth University Park, PA 16802-7501
1	Pennsylvania State University Department of Mechanical Engineering ATTN: K. Kuo University Park, PA 16802-7501
1	Purdue University School of Mechanical Engineering ATTN: J. R. Osborn TSPC Chaffee Hall West Lafayette, IN 47907-1199

No. of Copies	Organization
1	SRI International Propulsion Sciences Division ATTN: Technical Library 333 Ravenwood Avenue Menlo Park, CA 94025-3493
1	Rensselaer Ploytechnic Institute Department of Mathematics Troy, NY 12181
2	Director Los Alamos Scientific Laboratory ATTN: T3, D. Butler M. Division, B. Craig P. O. Box 1663 Los Alamos, NM 87544
1	General Applied Sciences Laboratory ATTN: J. Erdos 77 Raynor Avenue Ronkonkama, NY 11779-6649
1	Battelle PNL ATTN: Mr. Mark Garnich P. O. Box 999 Richland, WA 99352
1	Stevens Institute of Technology Davidson Laboratory ATTN: R. McAlevy, III Castle Point Station Hoboken, NJ 07030-5907
1	Rutgers University Department of Mechanical and Aerospace Engineering ATTN: S. Temkin University Heights Campus New Brunswick, NJ 08903
1	University of Southern California Mechanical Engineering Department ATTN: 0HE200, M. Gerstein Los Angeles, CA 90089-5199
2	University of Utah Department of Chemical Engineering ATTN: A. Baer G. Flandro Salt Lake City, UT 84112-1194

No. of Copies	Organization
1	Washington State University Department of Mechanical Engineering ATTN: C. T. Crowe Pullman, WA 99163-5201
1	Honeywell, Inc. ATTN: R. E. Tompkins MN38-3300 10400 Yellow Circle Drive Minnetonka, MN 55343
1	Science Applications, Inc. ATTN: R. B. Edelman 23146 Cumorah Crest Drive Woodland Hills, CA 91364-3710
	Aberdeen Proving Ground
	Cdr, CSTA ATTN: STECS-LI, R. Hendricksen

No. of Copies	Organization
1	Ernst-Mach-Institut ATTN: R. Heiser Abteilung fur Ballistik Hauptstrasse 18 7858 Weil am Rhein Germany
1	Defence Research Centre Salisbury ATTN: Dr. S.E. Stephenson G.P.O. Box 2151 Adelaide South Australia 5001
1	US Army Research, Development and Standardization Group (UK) ATTN: Dr. Roy Reichenbach 223 Old Marylebone Rod London NW1 5TH England
1	Royal Armament R&D Establishment ATTN: C. Woodley Fort Halstead Sevenoaks Kent TN14 7BP England
1	Defence Research Establishment Valcartier ATTN: Ms. J. Maillette 2459 Pie XI Blvd., North (P.O. Box 8800) Courcellette, Quebec, G0A 1R0 Canada

USER EVALUATION SHEET/CHANGE OF ADDRESS

This Laboratory undertakes a continuing effort to improve the quality of the reports it publishes. Your comments/answers to the items/questions below will aid us in our efforts.

1. BRL Report Number BRL-TR-3102 Date of Report May 90

2. Date Report Received _____

3. Does this report satisfy a need? (Comment on purpose, related project, or other area of interest for which the report will be used.) _____

4. Specifically, how is the report being used? (Information source, design data, procedure, source of ideas, etc.) _____

5. Has the information in this report led to any quantitative savings as far as man-hours or dollars saved, operating costs avoided, or efficiencies achieved, etc? If so, please elaborate. _____

6. General Comments. What do you think should be changed to improve future reports? (Indicate changes to organization, technical content, format, etc.) _____

CURRENT ADDRESS

Name

Organization

Address

City, State, Zip Code

7. If indicating a Change of Address or Address Correction, please provide the New or Correct Address in Block 6 above and the Old or Incorrect address below.

OLD ADDRESS

Name

Organization

Address

City, State, Zip Code

(Remove this sheet, fold as indicated, staple or tape closed, and mail.)

FOLD HERE

DEPARTMENT OF THE ARMY
Director
U.S. Army Ballistic Research Laboratory
ATTN: SLCBR-DD-T
Aberdeen Proving Ground, MD 21[illegible]-5066
OFFICIAL BUSINESS

NO POSTAGE
NECESSARY
IF MAILED
IN THE
UNITED STATES

BUSINESS REPLY MAIL
FIRST CLASS PERMIT No 0001, APG, MD

POSTAGE WILL BE PAID BY ADDRESSEE

Director
U.S. Army Ballistic Research Laboratory
ATTN: SLCBR-DD-T
Aberdeen Proving Ground, MD 21005-9989

FOLD HERE